

Digital Breast Tomosynthesis: State of the Art¹

Srinivasan Vedantham, PhD
Andrew Karellas, PhD
Gopal R. Vijayaraghavan, MD, MPH
Daniel B. Kopans, MD

Online SA-CME

See www.rsna.org/education/search/ry

Learning Objectives:

After reading the article and taking the test, the reader will be able to:

- Discuss the rationale for the use of digital breast tomosynthesis—its advantages, limitations, and the importance of results from major clinical studies
- Recognize the differences between the various technological approaches to digital breast tomosynthesis
- Demonstrate the potential of digital breast tomosynthesis in improving the confidence for diagnosis

Accreditation and Designation Statement

The RSNA is accredited by the Accreditation Council for Continuing Medical Education (ACCME) to provide continuing medical education for physicians. The RSNA designates this journal-based SA-CME activity for a maximum of 1.0 *AMA PRA Category 1 Credit*[™]. Physicians should claim only the credit commensurate with the extent of their participation in the activity.

Disclosure Statement

The ACCME requires that the RSNA, as an accredited provider of CME, obtain signed disclosure statements from the authors, editors, and reviewers for this activity. For this journal-based CME activity, author disclosures are listed at the end of this article.

¹ From the Department of Radiology, University of Massachusetts Medical School, 55 Lake Ave North, Worcester, MA 01655 (S.V., A.K., G.R.V.); and Department of Radiology, Massachusetts General Hospital, Harvard Medical School, Boston, Mass (D.B.K.). Received June 13, 2014; revision requested July 18; revision received December 19; final version accepted December 30.

Address correspondence to A.K. (e-mail: andrew.karellas@umassmed.edu).

The contents are solely the responsibility of the authors and do not reflect the official views of the National Institutes of Health or the National Cancer Institute.

© RSNA, 2015

This topical review on digital breast tomosynthesis (DBT) is provided with the intent of describing the state of the art in terms of technology, results from recent clinical studies, advanced applications, and ongoing efforts to develop multimodality imaging systems that include DBT. Particular emphasis is placed on clinical studies. The observations of increase in cancer detection rates, particularly for invasive cancers, and the reduction in false-positive rates with DBT in prospective trials indicate its benefit for breast cancer screening. Retrospective multi-reader multicase studies show either noninferiority or superiority of DBT compared with mammography. Methods to curtail radiation dose are of importance.

© RSNA, 2015

Screening asymptomatic women for breast cancer with mammography in conjunction with advances in therapy have shown to reduce breast cancer-related mortality (1–5). The sensitivity of screen-film mammography for the detection of breast cancer varies with breast density and is lower for women with heterogeneously dense or extremely dense breasts (6–8). The positive predictive value (PPV2) of findings recommended for biopsy range from 20% to 40%, with a median of 31.4% (9). Over the past decade, mammography has transitioned from screen-film systems to digital detectors (10–12). Full-field digital mammography (FFDM) compared with screen-film mammography improved the diagnostic accuracy in certain sub-

groups of women, including women 49 years of age or younger and those with dense breasts (13). Among women who are screened annually, the median recall rate is approximately 9.3% in the United States (14). Major contributors to recall are breast density that can obscure a lesion and superimposition of fibroglandular tissue that can be misinterpreted as a lesion when none is present. Tissue superposition creates a masking effect, referred to as “anatomical noise” in literature, which limits lesion detection, particularly soft-tissue abnormalities (15). Digital breast tomosynthesis (DBT) (16), a limited-angle tomographic breast imaging technique, was developed to overcome tissue superposition and its clinical adaptation was facilitated by the development of digital detectors.

In DBT, multiple projection views are acquired while the x-ray source traverses along a predefined trajectory, typically an arc spanning an angular range of 60° or less, and the acquired projection views are reconstructed to provide sections parallel to the breast support. While the general concept of tomosynthesis for radiographic imaging dates back to early 1930s (17), it was invented for breast imaging in the 1990s (18). In 1997, the landmark article by Niklason et al (16) demonstrated the feasibility of digital tomosynthesis for breast imaging using mastectomy specimens. A comprehensive review of digital x-ray tomosynthesis for chest and breast imaging applications was provided by Dobbins and Godfrey (19). Specific to breast imaging, there have been several reviews addressing the advancements (20–23), clinical applications of DBT (24–29), and advancements in DBT technology (30,31). Also, a recent article chronicled the transition of DBT from an imaging concept to the clinic from the perspective of an inventor (32). A search of the PubMed database identified more than 100 research articles on this topic since 2012. Hence, this review is provided with the intent of describing the state of the art in terms of technology, results from recent clinical studies, advanced applications such as contrast media-enhanced DBT, and ongoing efforts to develop multimodality imaging systems that include DBT.

Imaging Systems

Current clinical and clinical-prototype DBT systems differ in imaging geometry, angular range of x-ray tube motion, number of projections and distribution, scan duration, acquisition method such as step-and-shoot or continuous x-ray motion, detector technology and its operation such as pixel binning, and reconstruction algorithms. Table 1 provides a summary of the specifications for some of the clinical DBT systems that have European regulatory (CE mark) approvals and at least three of these systems have U.S. Food and Drug Administration approval. DBT systems have also been developed by Sectra Mamea AB (Linköping, Sweden) now part of Philips Healthcare (Best, the Netherlands), Fujifilm (Tokyo, Japan), Planmed Oy (Helsinki, Finland), and XCounter AB (Danderyd, Sweden). Specifications for these systems are provided by Sechopoulos (30) and in the draft version of the quality control protocol by European Reference Organization for Quality Assured Breast Screening and Diagnostic Services (33).



Imaging Geometry

Current clinical-prototype and clinical DBT systems utilize differing imaging system geometries and four of these approaches are shown in Figure 1. In

Essentials

- Current clinical and clinical-prototype digital breast tomosynthesis (DBT) systems differ in imaging geometry, angular range of tube motion, number of projections, scan duration, acquisition method such as step-and-shoot or continuous x-ray motion, detector technology and its operation such as pixel binning, and reconstruction algorithms.
- Studies in screening populations show a statistically significant reduction in recall rate with two-view DBT plus full-field digital mammography (FFDM) compared with two-view FFDM.
- Prospective trials in screening population from Europe show a statistically significant increase in cancer detection rate with two-view DBT plus FFDM compared with two-view FFDM, and retrospective observational studies from the United States show either a significant or a nonsignificant increase.
- Retrospective reader studies show either noninferiority or superiority of DBT compared with mammography in terms of area under the curve or other equivalent figures of merit.

Published online

10.1148/radiol.2015141303 Content code:  

Radiology 2015; 277:663–684

Abbreviations:

AUC = area under the curve
 BIRADS = Breast Imaging Reporting and Data System
 CAD = computer-aided detection
 CC = craniocaudal
 DBT = digital breast tomosynthesis
 FFDM = full-field digital mammography
 MGD = mean glandular dose
 MLO = mediolateral oblique
 ROC = receiver operating characteristic
 SM = synthesized 2D mammography
 2D = two-dimensional

Funding:

This research was supported by the National Institutes of Health (grants R01 CA139449 and R21 CA176470).

Conflicts of interest are listed at the end of this article.

Table 1

Specifications of Clinical DBT Systems

Manufacturer	General Electric*	Hologic	Internazionale Medico Scientifica	Siemens
Model/platform	SenoClaire/Senographe Essential	Selenia Dimensions	Giotto Tomo	MAMMOMAT Inspiration
Source to detector distance (cm)	66	70	68	65.5
Source to center-of-rotation distance (cm)	62	70	66	60.8
Source to breast support distance (cm)	63.8	67.5	65.8	63.8
X-ray tube angular range	$\pm 12.5^\circ$	$\pm 7.5^\circ$	$\pm 20^\circ$	$\pm 25^\circ$
X-ray tube motion	Step-and-shoot	Continuous	Step-and-shoot	Continuous
Detector angular range	Stationary	$\pm 2.1^\circ$	Stationary	Stationary
X-ray tube target material(s)	Mo/Rh	W	W	W
X-ray filter material(s)	Mo/Rh	Al	Rh/Ag	Rh
No. of projections	9	15	13	25
Equiangular distribution of projections	Yes	Yes	No [†]	Yes
Scan time (sec)	Typically <10	3.7	12	25
Detector type	a-Si indirect conversion	a-Se direct conversion	a-Se direct conversion	a-Se direct conversion
Detector pixel size (μm) [‡]	100	70 (2×2 binned)	85	85
Equal milliamperere-second/projection	Yes	Yes	No [§]	Yes
Reconstruction method	Iterative (ASiR-DBT)	FBP/iterative contrast	Iterative	FBP/section thickness filter

Note.—Clinical prototypes have been developed by Sectra Mamea AB now part of Philips Healthcare, Fujifilm, Planmed Oy and XCounter AB. a-Se = amorphous selenium, a-Si = amorphous silicon, FBP = filtered back-projection.

* System uses a 5:1 linear antiscatter grid with focal distance of 65 cm.

[†] Finer angular sampling near central (0°) projection.

[‡] Pixel size prior to binning.

[§] Approximately 50% of total milliamperere-second to 0° degree projection and the remainder distributed evenly over the 12 projections. Data compiled from references 30,33 and from manufacturer provided information.

Figure 1, A, the detector may also be angulated with respect to the center of rotation while the x-ray source traverses an arc in a predetermined ratio and is referred to as isocentric motion of the detector. In one such system, the detector is angulated by $\pm 2.1^\circ$ while the x-ray source traverses $\pm 7.5^\circ$. In Figure 1, B, the detector remains stationary, while the x-ray source traverses an arc and is similar to the approach used in the feasibility study (16). In Figure 1, C, the approach is similar to Figure 1, B, with the range of x-ray tube movement covering a larger angle. At least one system allows user-selectable modes that also control the angular range of x-ray tube movement. A slot-scan DBT system (Fig 1, D), in which the center of rotation is located below the detector, has been developed (34). Another slot-scan DBT system uses linear tomosynthesis, in which the x-ray tube and detector are translated in a linear manner instead of the arc motion.

Each approach has its benefits and potential limitations. In the stationary

detector geometry (Fig 1, B and C), the thickness of the detector assembly can be minimal and may allow for improvement in patient positioning. Oblique x-ray incidence on the detector at large x-ray source angles can reduce spatial resolution in acquired projections (35,36). While it is possible to model this effect (37–39), it is unclear if corrections, either by processing the projections prior to reconstruction or as part of the reconstruction process, have been implemented. Additionally, the detector needs to be sufficiently large in the lateral direction so that the breast periphery is included in acquired projections to minimize truncation. Systems using isocentric motion of the detector to reduce blurring due to oblique x-ray incidence (Fig 1, A) need to provide sufficient mechanical clearance for the detector motion. The thickness of the detector assembly can be reduced by shifting the center of rotation to the detector plane, resulting in detector tilt with x-ray source angle, and by using a

smaller ratio of the detector to the x-ray source angulation. Slot-scan geometry has excellent x-ray scatter rejection properties. In one such implementation, the system used 21 photon-counting line detectors and the tomography angle was 11° (34). In another implementation of slot-scan geometry, the system used 48 line detectors and the breast is scanned in a linear manner over 18 seconds (40).

While adapting a FFDM system for DBT appears straightforward, there are several design aspects that need to be considered. The x-ray tube assembly and the patient face protective shield must be ensured not to interfere with patient positioning and not to strike the patient during tube motion. The mechanical design needs to minimize vibration and provide for high precision. Lack of precision among projections can cause substantial reduction in lesion contrast (41). Asymmetric x-ray beam collimation that varies during the scan is needed to ensure that the x-ray field is restricted to the detector. Clin-

Figure 1

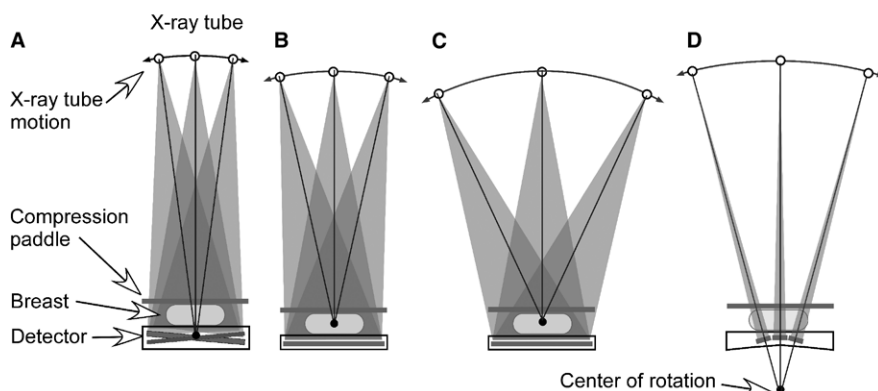


Figure 1: Clinical DBT systems vary in imaging system geometry and some of these approaches are shown. *A*, Detector is angulated with respect to the center of rotation while the x-ray source traverses an arc in a predetermined ratio and is referred to as isocentric motion of detector. *B,C*, Detector remains stationary, while the x-ray source traverses an arc covering a predetermined angular range, with the x-ray tube covering a larger angle in *C* than in *B*. *D*, A slot-scan DBT system is shown, in which the center of rotation is located below the breast.

ical DBT systems use either step-and-shoot acquisition, in which the x-ray tube moves to a predetermined position (angle), acquires the projection, and then proceeds to the next position, or continuous x-ray tube movement. The former approach avoids blurring due to x-ray focal spot motion within each projection but requires appropriate mechanical design for stop-start motion of the gantry. In the latter approach, x-ray focal spot motion within each projection results in resolution degradation. This can be partly mitigated by using pulsed x-ray source with as small a pulse-width as possible.

In general, the larger angular range of the x-ray tube motion results in more tomographic information yielding better section separation or vertical (*z*-axis) resolution. An increase in the angular range for the tube motion requires an increase in the number of projections for sufficient sampling (42,43). The need to acquire multiple projections in the shortest possible timeframe to minimize the likelihood for patient motion requires detector design with suitable temporal characteristics in terms of rapid signal readout and minimal image lag. To maintain the radiation dose to the breast from DBT at levels comparable to mammography, the x-

ray tube output is divided over multiple projections, so that each projection delivers a fraction of the radiation dose. This requires detectors with high detective quantum efficiency at low air kerma or exposure levels. Hence, detectors were specifically configured for DBT imaging (44–46). Current clinical DBT systems in the United States use either indirect conversion CsI:Tl scintillator coupled amorphous silicon detectors with a pixel pitch typically of 100 μm (46) or direct conversion amorphous selenium detectors (12,47). Depending on the manufacturer, amorphous selenium-based DBT systems use a detector with a native pixel pitch of 65–85 μm (12,47–50). Such systems are operated in full resolution (47–50), in 2×2 binned mode (12,49,50), or in 2×1 asymmetric binned mode (47,48), where the binning in the asymmetric mode is along the x-ray source movement direction. The use of pixel binning allows for faster detector readout, albeit at reduced spatial resolution. One amorphous selenium-based DBT system (49,50) uses hexagonal pixels that increase the proportion of pixel area sensitive to x-rays and allows user-selectable modes that control pixel binning and x-ray tube angular range. In that system, the angular range can be

selected to be $\pm 7.5^\circ$ or $\pm 20^\circ$, takes 4 or 9 seconds for acquisition, and provides reconstructed in-plane pixel size of 150 or 100 μm (33,50). For detectors employing hexagonal pixels, the pixel spacing along the two orthogonal directions vary and require resampling to square pixels to suit grayscale displays. In theory, the hexagonal pixels can be resampled to square pixels of any desired pitch.

Image Reconstruction

In the first study (16), a clinical-prototype FFDM system (GE Global Research, Niskayuna, NY) was modified to acquire nine projections over an x-ray source angular range of 40° followed by reconstruction using a linear shift-and-add algorithm. Suryanarayanan et al (51,52) modified a similar FFDM clinical prototype (11) to acquire seven projections over a 36° range to investigate the contrast-detail characteristics of tuned-aperture computed tomography reconstruction algorithm developed by Webber and his colleagues (53,54) and a maximum likelihood-based iterative reconstruction algorithm. Tuned-aperture computed tomography is similar to shift-and-add algorithm and uses radio-opaque fiducial markers to determine the geometry from projections. Improvement in contrast-detail characteristics with DBT compared with FFDM was observed in both studies (51,52). Wu et al (55) investigated back-projection that is similar to shift-and-add algorithm, filtered back-projection that is routinely used in computed tomography, and maximum likelihood algorithms with phantoms and clinical images. The study observed trade-offs between back-projection and filtered back-projection, with back-projection providing higher signal difference-to-noise ratio for low-contrast objects (masses) but with substantial out-of-plane artifacts and filtered back-projection providing an improvement in visualizing microcalcifications (55). Overall, maximum likelihood provided better balance for both masses and microcalcifications compared with the other two algorithms (55). Chen et al (56) noted the need to account for the shift in the direction orthogonal

to x-ray tube movement during back-projection. Several investigations into modeling (57–59) and optimizing filter kernels (60–62) used during filtered back-projection reconstruction have been reported.

Another class of algorithms utilizes linear algebra for reconstruction. Specific to DBT, simultaneous algebraic reconstruction (63,64) and matrix-inversion tomosynthesis (65) have been investigated. Simultaneous algebraic reconstruction with selective diffusion-based regularization (noise reduction) was shown to improve the contrast-to-noise ratio while preserving the sharpness of microcalcifications (64). Gaussian frequency blending of filtered back-projection and matrix-inversion tomosynthesis was shown to provide better reconstruction of microcalcifications with less high-frequency noise than filtered back-projection and better low-frequency content than matrix inversion tomosynthesis (65). Several additional algorithms (eg, 66–69) have been investigated for DBT reconstruction.

A few general inferences can be made regarding reconstruction algorithms with the understanding that the systems used in aforementioned studies varied in terms of the imaging geometry, the angular range of x-ray source movement, and the detector characteristics that could substantially affect image quality. Traditional back-projection reconstruction and similar techniques such as shift-and-add algorithm and tuned-aperture computed tomography have largely been replaced by other algorithms, partly due to substantial out-of-plane artifacts. The choice of filter kernel has a substantial effect on DBT reconstructions with filtered back-projection. In general, filtered back-projection accentuates high-frequency content on reconstructed images owing to the use of a ramp filter, and the high-frequency noise on reconstructed images can be controlled to some extent with an appropriate apodization filter. Filtered back-projection requires less computational effort compared with maximum likelihood or other iterative reconstruction techniques. Maximum likelihood and several other statisti-

cal iterative reconstruction algorithms can tolerate higher image noise in projections. Simultaneous algebraic reconstruction can provide for faster reconstruction than maximum likelihood and can achieve image quality comparable to maximum likelihood. Dobbins and Godfrey (19) and Sechopoulos (31) have provided comprehensive reviews of DBT reconstruction algorithms.

Radiation Dose

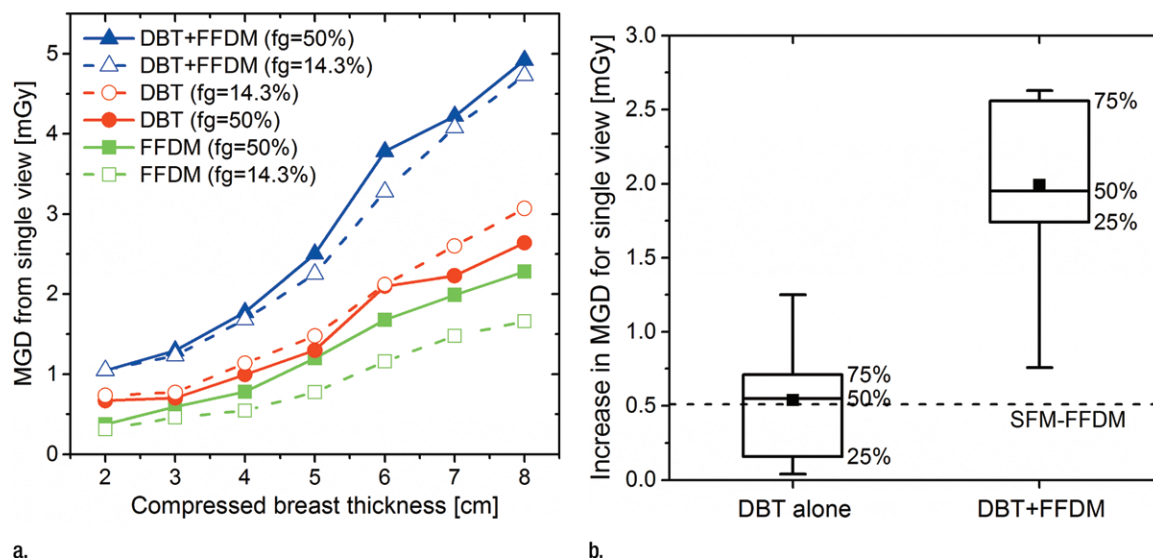
Radiation dose to the breast from x-ray imaging examinations is reported using the mean glandular dose (MGD) metric, which apportions the dose to the at-risk fibroglandular breast tissue (70). MGD is determined from measurement of air kerma (or exposure) incident on the breast or a breast-equivalent phantom, followed by scaling using a Monte Carlo simulation-derived conversion factor, referred to as normalized glandular dose coefficient that is specific to the x-ray beam quality. The variation in the normalized glandular dose coefficient with x-ray tube angle relative to the central projection (0°), referred to as relative glandular dose, was weakly dependent on fibroglandular fraction and x-ray spectrum and showed a larger dependence on breast size and thickness in mediolateral oblique (MLO) view compared with craniocaudal (CC) view (71). Patient positioning, particularly for MLO view, was reported to cause a 5%–13% variation in MGD (72). While the initial study (71) was based on a DBT system using molybdenum or rhodium target x-ray tube, subsequent studies addressed tungsten target x-ray tubes (72,73). Currently, many DBT systems use tungsten target with aluminum, silver, or rhodium filter (Table 1) and operate at a slightly higher applied tube voltage (kilovolts peak) than FFDM, partly to reduce radiation dose to the breast.

Dosimetry protocols used in the United States differ from United Kingdom, European, and IAEA (International Atomic Energy Agency) protocols in terms of assumptions pertaining to fibroglandular fraction and skin layer thickness and its composition (74,75). Dance et al (76) provided a DBT system-specific factor in determining

MGD as per United Kingdom, European, and IAEA protocols. A recent task group report from the American Association of Physicists in Medicine provided similar factors for each DBT system (77). Dosimetry of a system capable of DBT and FFDM acquisitions using the automated exposure control mechanism showed that in general, the MGD from DBT was higher than that from FFDM (77). For the combined DBT plus FFDM mode (hereafter, DBT-FFDM), the MGD determined as per dosimetry protocol used in the United States was lower than the regulatory limit of 3 mGy for a CC-equivalent view of an average breast (78). Data provided in that report (78) showed that for the same compressed breast thickness, the ratio of the MGD from DBT to that from FFDM showed a decreasing trend with increasing glandular fraction. The study also showed (78) that the MGD from FFDM and DBT for a single view increased with increasing breast thickness and was used to construct the plots for 50% and 14.3% fibroglandular breasts in Figure 2a. A 50% fibroglandular breast corresponds to the assumed average breast composition used in United States protocol and a 14.3% fibroglandular breast corresponds to approximately average realistic composition reported in recent studies (79–82). It is relevant to note that the estimated MGD is with automatic exposure control, and for the desired image quality, the technique factors and consequently the MGD can be chosen.

Several independent studies (34,83–87) have reported the MGD for single view from FFDM and DBT and were used to construct the box plot shown in Figure 2b. Within each study, the FFDM and DBT systems were matched by vendor, if MGD from multiple FFDM systems were reported. Compared with FFDM, the median increase in the MGD for single view with DBT is similar to the slightly higher dose with screen-film mammography (88). It is arguable if this constitutes a meaningful increase in radiation-associated risk (89). However, there is approximate 2 mGy increase with DBT-FFDM compared with FFDM alone (Fig 2b). This constitutes an approximate doubling of the MGD

Figure 2



a.

b.

Figure 2: (a) MGD for a single CC-equivalent view from FFDM, DBT, and the combined DBT-FFDM provided in reference 78 for various compressed breast thicknesses and for 50% and 14.3% fibroglandular breasts (*fg*) are shown. (b) Box plot of the increase in MGD from a single view, in units of milligrays, with respect to FFDM, due to DBT alone and the combined DBT-FFDM study. Symbol within each box is the mean and the whiskers the maximum and minimum. Dashed line = difference in MGD between screen-film mammography (*SFM*) and FFDM reported by the Digital Mammographic Imaging Screening Trial (DMIST) study (88). Data for **b** were compiled from references 34,83–87. Within each study, the FFDM and DBT systems were matched by vendor, if MGD from multiple FFDM systems were reported.

as detailed in a recent review on the radiation dose from DBT (90). One possible manner to limit the radiation dose to the breast is by using synthesized two-dimensional (2D) mammograms (SMs) from DBT (91,92), rather than acquiring an additional mammogram. DBT plus SM (hereafter, DBT-SM) can reduce the MGD by approximately 45% compared with DBT-FFDM (90). An alternative approach is to apportion a larger fraction of the x-ray tube output to the central (0°) projection during the DBT scan and to use this projection as a digital mammogram (93,94). One system apportions approximately 50% of the x-ray tube output to the central (0°) projection, with the remainder distributed over other projections (Table 1).

In summary, there is wide variability in technological approaches used in current clinical and clinical-prototype DBT systems. At present there is limited information on comparative evaluation of these approaches using objective physics-based metrics (33), and more importantly comparative clinical studies are

lacking. Such studies can provide a better understanding of the relative merits of these approaches.

Clinical Studies

There have been several clinical studies investigating DBT either alone or as an adjunct to FFDM. We broadly classified these investigations as studies in screening populations, studies in diagnostic populations, retrospective reader studies, and studies intended for clinical management following diagnosis.

Studies in Screening Populations

Table 2 provides a summary of studies comparing FFDM alone with DBT-FFDM in screening populations. Two studies were prospective clinical trials from Europe (the OTST [Oslo Tomosynthesis Screening Trial] and the STORM [Screening with Tomosynthesis or Mammography] trial) that follow a biennial screening program as per European guidelines and two were retrospective studies from the United States that report on their observations of

screening performance metrics after introduction of DBT in routine clinical practice.

The OTST is a four-arm study comparing FFDM, adjunctive use of computer-aided detection (CAD) to FFDM (FFDM-CAD), DBT-FFDM, and DBT-SM in women 50–69 years of age from which interim analyses with 12621 women have been reported (86,95). Consenting women underwent bilateral two-view combined DBT-FFDM examination. For each arm of the study, one of eight radiologists independently interpreted the images. Unless all four interpretations were negative or definitely benign, consensus-based arbitration with at least two radiologists was used to determine if the patient needed to be recalled. The prearbitration scores were used to determine the false-positive rate and the cancer detection rate attributable to each arm. Compared with FFDM, DBT-FFDM increased the cancer detection rate from 6.1 to 8.0 per 1000 and decreased the prearbitration false-positive rate from 6.1% to 5.3%, which were significant after adjusting for

Table 2

Clinical Studies Comparing FFDM with DBT-FFDM in Screening Population

Study and Reference No.	Study Design	Key Results
OTST trial (86,95)	Four-arm prospective study comparing FFDM, FFDM-CAD, DBT-FFDM, and DBT-SM. Subjects underwent combined DBT-FFDM examination. Independent reading by four radiologists, one for each arm, followed by arbitration.	DBT-FFDM vs FFDM ($n = 12,621$): DBT-FFDM, -reduced prearbitration FPR from 6.1% to 5.3% -increased CDR from 6.1 to 8.0 -detected 25 additional invasive cancers Paired double-read-(DBT-FFDM; DBT-SM) vs (FFDM; FFDM-CAD) ($n = 12,621$): In DBT arm, -Prearbitration FPR reduced from 10.3% to 8.5% -CDR increased from 7.1 to 9.4 -27 additional invasive cancers detected
STORM trial (96)	Prospective study comparing FFDM vs DBT-FFDM. Subjects underwent combined DBT-FFDM examination. Sequential double reading of FFDM followed by DBT-FFDM.	DBT-FFDM vs FFDM ($n = 7292$): In DBT arm, -Estimated FPR reduction of 17% -CDR increased from 5.3 to 8.1 -20 additional cancers detected
Malmö Breast Tomosynthesis Screening Trial (103)	Prospective study comparing one-view (MLO) DBT vs two-view FFDM. Subjects underwent both examinations. Independent reading for each arm followed by arbitration. (Interim results)	One-view DBT vs two-view FFDM ($n = 7,500$): In DBT arm, -CDR increased from 6.3 to 8.9 -20 additional cancers detected -Recall rate increased from 2.6% to 3.8%
Rose et al (98)	Retrospective observational study before and after introduction of DBT in clinic. Subjects self-elected to undergo DBT-FFDM.	FFDM ($n = 13,856$) vs DBT-FFDM ($n = 9,499$): For subjects in DBT-FFDM group, -RR reduced from 8.7% to 5.5% -PPV1 increased from 4.7% to 10.1% -Nonsignificant increase in CDR from 4.0 to 5.4
Haas et al (101)	Retrospective observational study. Subjects underwent DBT-FFDM based on system availability.	FFDM ($n = 7058$) vs DBT-FFDM ($n = 6100$): For subjects in DBT-FFDM group, -RR reduced from 12.0% to 8.4% -RR reduced for women <70 years of age and BIRADS breast density ≥ 2 . -Nonsignificant increase in CDR from 5.2 to 5.7
Friedewald et al (102)	Retrospective observational study before and after introduction of DBT from 13 academic and nonacademic sites.	FFDM ($n = 281,187$) vs DBT-FFDM ($n = 173,663$): For subjects in DBT-FFDM group, -RR reduced from 10.7% to 9.1% -PPV1 increased from 4.3% to 6.4% -Significant increase in CDR from 4.2 to 5.4.

Note.—BIRADS = Breast Imaging Reporting and Data System, CDR = cancer detection rate per 1000 screens, FPR = false-positive rate, PPV1 = positive predictive value for recalls in percentage, RR = recall rate in percentage.

reader-specific performance levels (95). The study noted that while all four arms were considered during the arbitration, limited follow-up data were available regarding interval cancers, thus providing relative performance levels. Of the 121 cancers detected from all four arms, 77 were detected at FFDM alone and 101 were detected at DBT-FFDM. Of the 29 cancers with radiologic finding of microcalcifications alone, 26 and 25 were detected at FFDM and DBT-FFDM, respectively. A key observation from the study was that use of DBT-FFDM detected 25 additional invasive cancers. A subsequent report (86) provided analysis of paired double-read comparing 2D imaging (ie,

FFDM, FFDM-CAD) with 2D imaging plus DBT (DBT-FFDM, DBT-SM) that simulates the European reading protocol. The analysis indicated that the 2D imaging plus DBT pair improved cancer detection rates from 7.1 to 9.4 per 1000, depicted 27 additional invasive cancers, and reduced false-positive rates from 10.3% to 8.5%. As noted by the authors, the study was not a pure double-read as within each pair, the modalities differed. However, it was noted that the effects within each pair were small compared with between pairs. The increase in the detection of invasive cancers is highly important.

The STORM trial compared FFDM with DBT-FFDM in 7292 women, 48

years of age or older, who attended the Verona and Trento screening services in Italy (96). Consenting participants underwent bilateral two-view combined DBT-FFDM examination. Each study was double-read by two of eight radiologists. Each radiologist sequentially read the FFDM study followed by the DBT-FFDM study. If either of the interpretations recommended recall then the subject was recalled. Fifty-nine cancers were detected in 57 women. All 59 cancers were detected with DBT-FFDM, whereas 39 cancers were detected with FFDM alone. Of the 20 additional cancers detected with DBT-FFDM, three were ductal carcinoma in situ and the remaining 17 were invasive

cancers. Compared with FFDM, DBT-FFDM improved the cancer detection rate from 5.3 to 8.1 per 1000. Similar to the OTST, the study had limited data on interval cancers, thus providing relative performance levels for the modalities. Of the 395 false-positive recalls, 68 would have been avoided if a positive screening from DBT-FFDM was the criterion for recall, reducing the false-positive rate by 17.2%. A subsequent analysis (97) of each screening service observed an increase in cancer detection rates with DBT-FFDM at both centers. The false-positive rates differed between the centers; the center with higher false-positive rate would have experienced a larger reduction if a positive screening from DBT-FFDM was the criterion for recall. Additional analysis (85) indicated that interreader variability improved with DBT-FFDM compared with FFDM.

Rose et al (98) reported their observations from a single site before and after introduction of DBT in routine clinical practice. The study reported screening performance measures from 13856 FFDM screenings before introduction of DBT (period 1) and 9499 screens with DBT-FFDM (period 2). Pooled data from six radiologists who interpreted at least 500 examinations during each of the two time periods indicated a statistically significant reduction in recall rate from 8.7% (FFDM alone, period 1) to 5.5% (DBT-FFDM, period 2) and a statistically significant increase in positive predictive value (PPV1) for recalls from 4.7% (FFDM alone, period 1) to 10.1% (DBT-FFDM, period 2). Cancer detection rate and invasive cancer detection rate showed a nonsignificant increase with DBT-FFDM compared with FFDM alone. Among women who underwent screening for the first time, the recall rates were 13.6% (FFDM alone, period 1) and 9.6% (DBT-FFDM, period 2), and the cancer detection rates were 4.1 and 7.7 per 1000 screening examinations. The authors noted that case selection bias could not be ruled out during period 2, as women self-elected to undergo the DBT-FFDM examination. Other retrospective observational studies have

also reported reduction in recall rate (99,100).

Haas et al (101) reported their observations from four sites over the same time period, of which two sites had DBT-FFDM for at least part of the period. Screening performance measures for 6100 women who underwent DBT-FFDM examination and 7058 women who underwent FFDM alone were reported. There was a significant reduction in the recall rate from 12.0% for women who underwent FFDM to 8.4% for women who underwent DBT-FFDM, and a nonsignificant increase in the cancer detection rate from 5.2 (FFDM alone) to 5.7 (DBT-FFDM) per 1000 screens. After adjusting for differences in subject characteristics (age, breast density, presence or absence of breast cancer risk factors) among the two study groups, a statistically significant 38% reduction in the recall rate was observed with DBT-FFDM. Recall rate reduction with DBT-FFDM was significant for all breast density categories with the exception of women with predominantly fatty breast, and for all age groups with the exception of women 70 years of age or older. In general, greater benefits in terms of odds for recall were observed for younger women and for women with dense breasts with DBT-FFDM compared with FFDM alone. Since this was a retrospective observational study where the choice of modality depended on system availability and patients could opt out of DBT-FFDM screening, the possibility of selection bias could not be ruled out and was noted by the authors.

A large retrospective study by Friedewald et al (102) reported their observations from 13 sites before and after introduction of DBT in clinical practice. The study reported screening performance measures from 281187 FFDM screenings before introduction of DBT (period 1) and 173663 screenings with DBT-FFDM (period 2). After adjusting for site effect to account for possible correlation between the two time periods within the same site, the study reported performance metrics such as recall rate, cancer detection rate including invasive and in situ cancer detection

rates, and positive predictive value for biopsies. Significant reduction in recall rate (9.1% vs 10.7%), increase in cancer detection (5.4 vs 4.2 per 1000), particularly for invasive cancers (4.1 vs 2.9 per 1000), and increase in positive predictive value for recall (6.4% vs 4.3%) were reported with DBT-FFDM compared with FFDM alone. The major strength of the study was the inclusion of data from both academic and non-academic sites. The authors noted that the possibility of selection bias could not be ruled out during study period 2 at sites that had both FFDM and DBT systems.

Figure 3 shows an example of false-positive reduction with DBT. In summary, studies in screening population show a statistically significant reduction in the recall rate with two-view DBT-FFDM compared with two-view FFDM. Prospective trials in screening populations from Europe show a statistically significant increase in the cancer detection rate with two-view DBT-FFDM compared with two-view FFDM, and retrospective observational studies from the United States show either a significant or a nonsignificant increase. All of the aforementioned studies lack complete follow-up data and hence preclude analysis of false-negative interpretations and consequently absolute sensitivity. All of the aforementioned studies used DBT systems from a single manufacturer and hence the variation in clinical performance due to system design cannot be inferred. Considering the substantial differences in technological approach among DBT system manufacturers and continuing technological developments, the availability of limited clinical data are challenging for a comprehensive analysis of the relative merits of these approaches. Further studies are needed to determine clinical outcomes. Interim results (103) from the Malmö Breast Tomosynthesis Screening Trial in Sweden, which is a prospective, paired, independent double-read study comparing one-view DBT with two-view FFDM, indicated an improvement in the cancer detection rate from 6.3 per 1000 (FFDM) to 8.9 per 1000 (DBT); however, the postarbi-

Figure 3

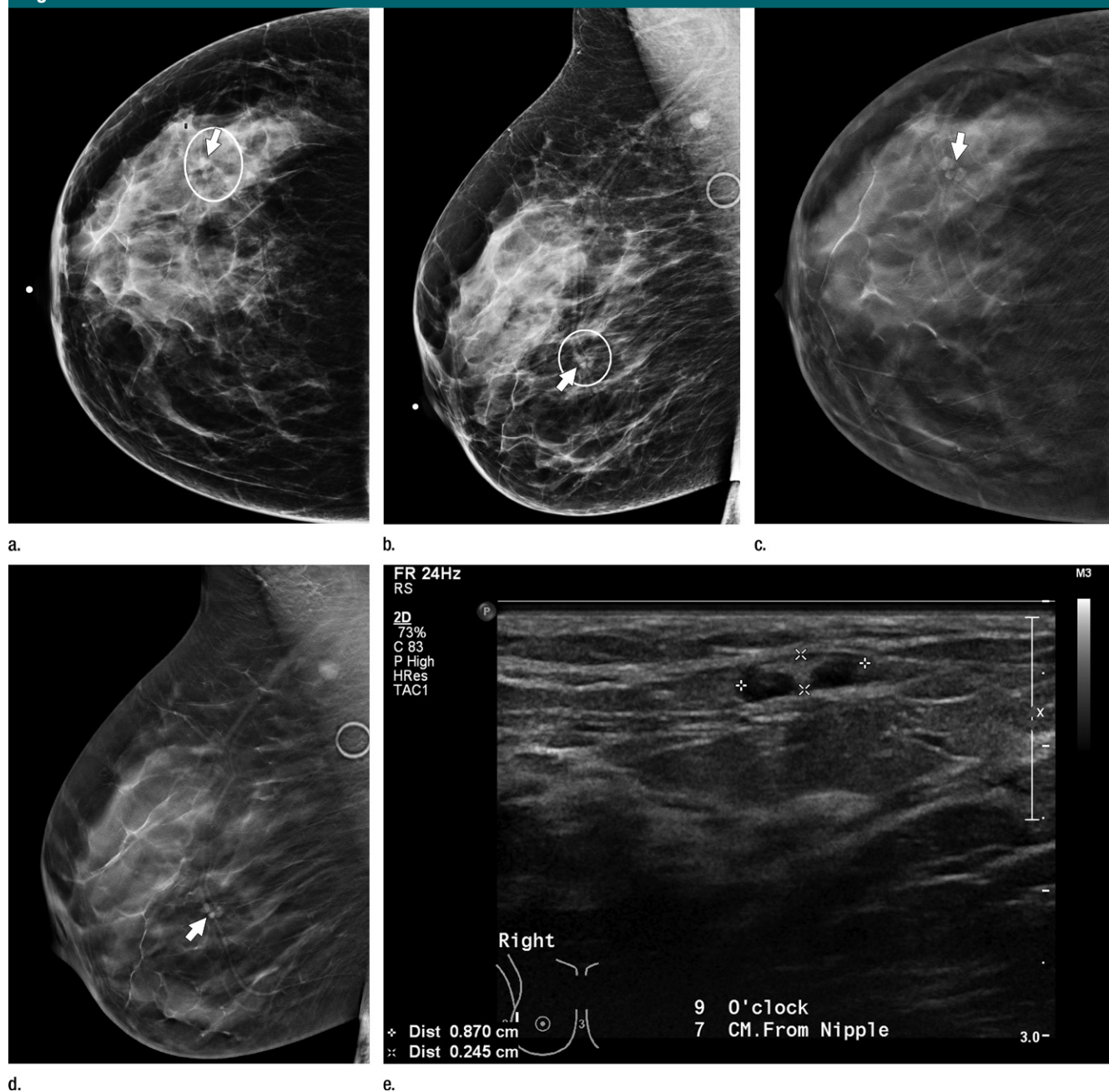


Figure 3: Images from combined DBT-FFDM screening in a 41-year-old woman with heterogeneous dense breasts. FFDM (a) CC and (b) MLO images of the right breast showed a lobulated mass at 9 o'clock (circle with arrow). (Additional circle in b = ring marker identifying a skin lesion.) Corresponding DBT (c) CC and (d) MLO images demonstrate this mass (arrow) to likely be a cluster of intramammary lymph nodes with fatty hila and confirming location just under the skin. That made (e) US evaluation easier and demonstrated the lymph nodes, and the woman was returned to screening.

tration recall rate increased from 2.6% (FFDM) to 3.8% (DBT). If DBT only increased the cancer detection rate without reducing the false-positive rate, then the recall rate will increase.

Studies in Diagnostic Populations

In a prospective study (104), 738 asymptomatic women recalled due to results at screen-film mammography underwent the combined two-view

DBT-FFDM examination. Each reader sequentially interpreted the screen-film mammography, FFDM, and DBT images in an unblinded manner reflective of clinical practice. The study reported

improvements in sensitivity, specificity, and predictive values with DBT. The area under the curve (AUC) improved from 0.788 for screen-film mammography to 0.895 with the addition of FFDM, and to 0.967 with further addition of DBT. The study reported that after the addition of DBT none of the malignant cases were classified as normal or benign.

Poplack et al (105) analyzed data from 98 FFDM-recalled women who underwent diagnostic evaluation using screen-film mammography and a DBT examination with a maximum of three views that was matched in orientation, but not magnification, with diagnostic mammography. Interpreting in an unblinded manner, in general, the clinical image quality for masses were either equivalent or superior, but microcalcifications were better visualized with diagnostic mammography. The observation with microcalcifications is likely due to the substantially higher spatial resolution of screen-film mammography compared with the prototype DBT employing pixel binning, the well-known advantage of magnified mammography views in terms of image sharpness, and the shorter exposure duration of mammography. The study estimated that 40% of the subjects would not have been recalled had DBT been used as an adjunct to FFDM screening.

In an another study, DBT imaging of 129 women after completion of standard-of-care diagnostic work-up and prior to biopsy (if recommended) prompted the recall of four women due to DBT findings, resulting in two invasive lobular carcinomas (106).

Waldherr et al (107) investigated MLO-view DBT in 144 FFDM-recalled or symptomatic women. Compared with two-view FFDM, consensus reading by two radiologists showed that DBT, either alone or adjunctively with FFDM, significantly improved sensitivity and negative predictive value. Comparing two-view FFDM with two-view DBT from 513 women with abnormal screening results or clinical symptoms, Teertstra et al (87) reported that DBT and FFDM were each false-negative for eight of 112 cancers. Combining the re-

sults from DBT and FFDM interpretations, 109 of 112 cancers were detected.

In a study of 146 women with 148 noncalcified abnormalities simulating diagnostic work-up using DBT (108), three readers retrospectively interpreted DBT studies along with the abnormal screening study and prior mammograms, blinded to the conventional diagnostic work-up. Concordance between the standard-of-care work-up and ratings from DBT interpretation in conjunction with breast ultrasonography (US), if indicated by readers, was assessed. The study suggested DBT can replace conventional diagnostic mammography for evaluation of noncalcified findings with similar sensitivity and specificity.

In summary, all of the studies show the benefit of DBT for diagnostic evaluation. Figure 4 shows an example in which DBT increased the confidence level for diagnosis. Figure 5 shows an example in which diagnostic work-up using DBT resolved an asymmetry noted with FFDM screening. Figure 6 shows an example in which DBT demonstrated not only the microcalcifications but also an associated irregular mass. However, some lesions may not be well visualized with DBT and an example is shown in Figure 7. Also, the presence of high-contrast objects such as surgical clips can cause substantial artifacts as shown in Figure 8. Algorithms are being developed to minimize these artifacts.

Retrospective Multireader Multicase Studies

Gur et al (109) compared two-view FFDM with two-view DBT alone and with two-view DBT-FFDM by using eight readers interpreting 125 breasts (unilateral examinations), of which 35 had cancers. Compared with FFDM, the study estimated false-positive recall rate reduction of 30% for the combined DBT-FFDM interpretation and a nonsignificant reduction for DBT interpretation. A subsequent free-response receiver operating characteristic (ROC) analysis (110) indicated a significant improvement in the summary performance metric with the combined DBT-FFDM interpretation.

Comparing MLO-view DBT with two-view FFDM of 376 breasts (63 cancers) from 197 women, Gennaro et al (111) concluded that DBT was noninferior to FFDM. A subsequent study (112), comparing the combination of MLO-view DBT and CC-view FFDM with two-view FFDM in 469 breasts (68 with cancers) from 235 women, also reached a similar conclusion. A free-response study (113) with six readers interpreting 463 breasts, of which 258 had one or more lesions, including 77 malignancies in 68 breasts, reported statistically significant improvements in lesion detection and lesion characterization with the combination of MLO-view DBT and CC-view FFDM compared with two-view FFDM.

Svahn et al (114) compared one-view DBT (88% MLO; 12% CC) with two-view FFDM of 185 breasts from 185 patients, of which 89 breasts had cancers. Five readers localized the findings and assigned BIRADS scale that was used for jackknife free-response ROC analysis. The highest rating for each breast was used in ROC analysis. The study reported that the reader-averaged AUC from ROC and the figure of merit from jackknife free-response ROC were significantly higher with one-view DBT compared with two-view FFDM.

Wallis et al (34) used a photon-counting DBT system and analyzed data from 130 women, all BIRADS breast density category 2 or higher, of whom 40 had cancers and 24 had benign lesions. All women underwent two-view DBT and two-view FFDM. Two reader studies were reported; a set of 10 readers interpreted two-view DBT and two-view FFDM, and another set of 10 readers interpreted MLO-view DBT and two-view FFDM. Compared with two-view FFDM, the AUC was not statistically different for MLO-view DBT and was significantly higher with two-view DBT. The AUC improvement with two-view DBT was significant for both masses and microcalcifications.

Rafferty et al (115) reported results from two retrospective reader studies from multi-institutional trials comparing the combined two-view DBT-FFDM with two-view FFDM. In one study, 312 cases (48 with cancer) were interpreted

Figure 4

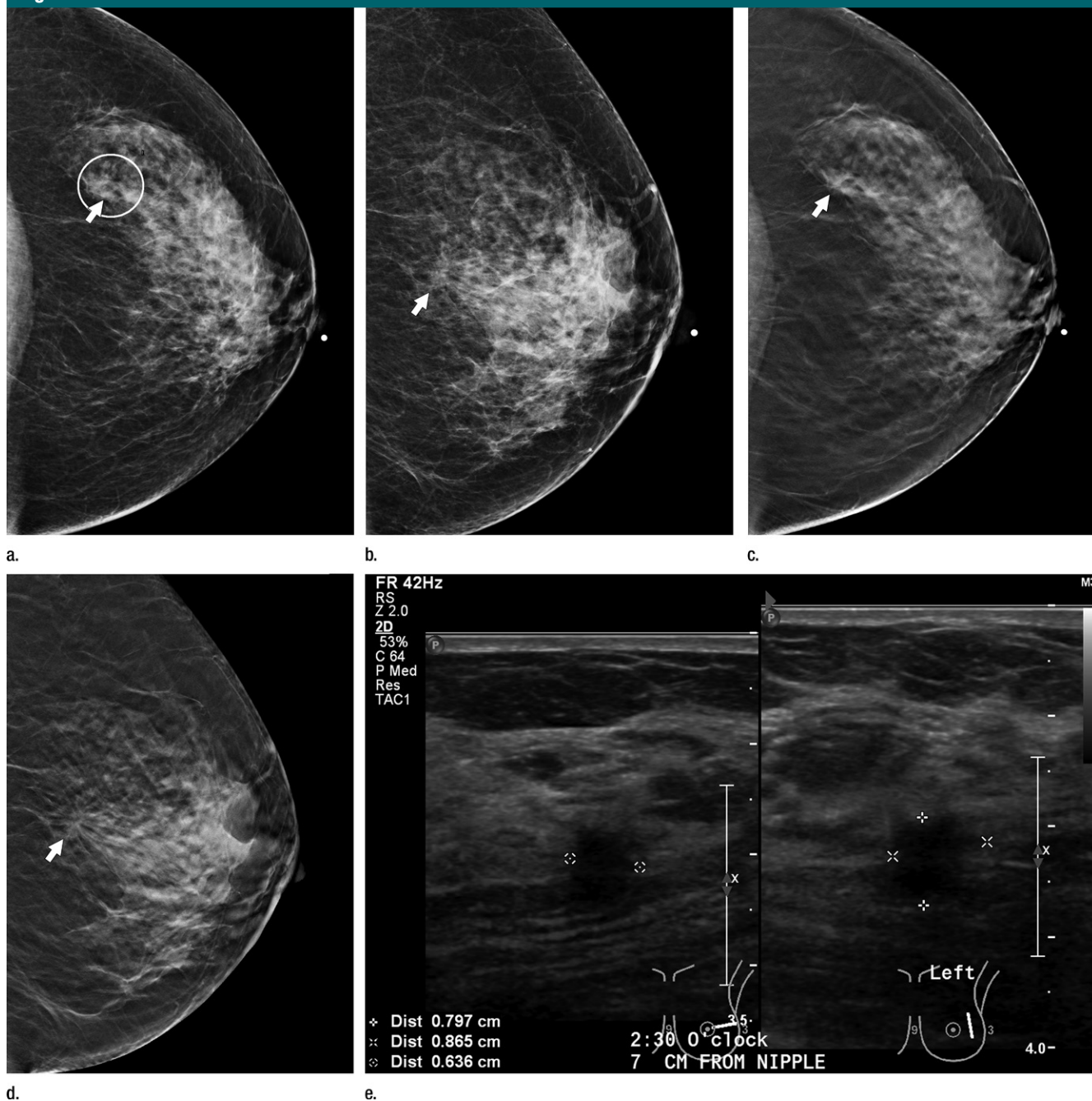


Figure 4: Images in 44-year-old woman who underwent combined DBT-FFDM after call back from FFDM screening that noted a focal asymmetry in the left breast. The asymmetry (arrow) could be noted on the (a) CC FFDM view and not well appreciated on the (b) mediolateral FFDM view. (c) CC and (d) MLO DBT views confirm a subtle spiculated lesion posteriorly in the upper outer quadrant. (e) US images confirm an 8-mm irregular hypoechoic solid mass. Mass was biopsied and pathologic evaluation verified invasive ductal carcinoma. DBT improved the confidence for diagnosis.

ed by 12 readers and in another study 310 cases (51 with cancer) were interpreted by 15 readers. DBT-FFDM sig-

nificantly improved AUC and reduced recall rates for noncancer cases in both reader studies. Sensitivity, particularly

for invasive cancers, improved with two-view DBT-FFDM. The study also reported that the improvement in AUC

Figure 5

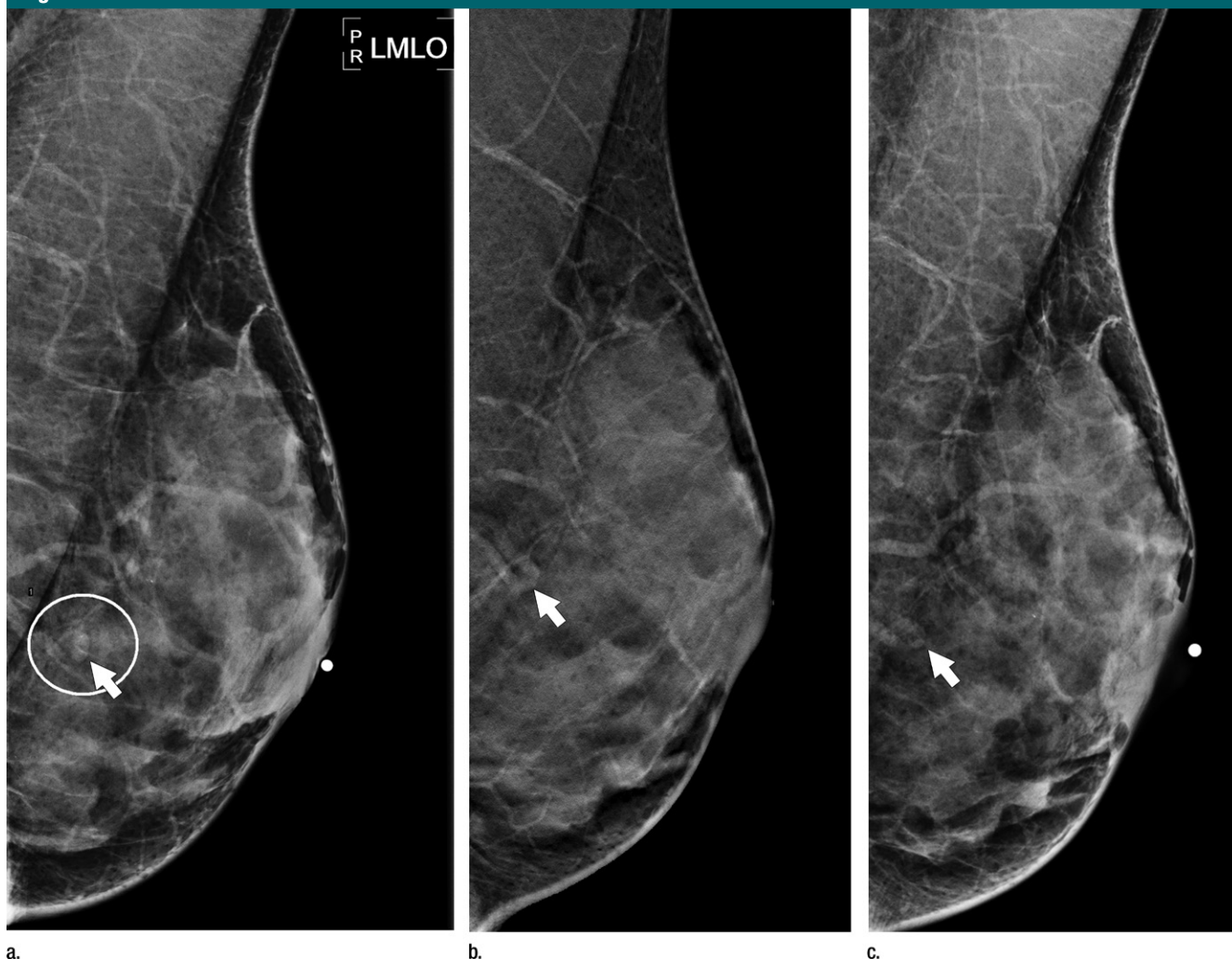


Figure 5: Images in a 52-year-old woman who was noted to have an asymmetry (arrow) on the (a) MLO view of the left breast at FFDM screening. (b) Diagnostic work-up with DBT confirmed a tortuous vessel accounting for the mammographic asymmetry and confidently returning the subject to annual screening. (c) The 1-year follow-up FFDM screening confirms DBT findings.

with DBT-FFDM was mostly for noncalcification cases.

Recent results from the TOMMY trial (a comparison of tomosynthesis with digital mammography) (116), which is a multicenter retrospective reader study comparing two-view FFDM alone, two-view DBT-FFDM, and two-view DBT-SM showed significant ($P < .001$) improvement in AUC for the DBT arms compared with FFDM alone. Most of the improvement was attributable to improved specificity ($P < .001$) with the DBT arms. There was a marginal, non-significant improvement in sensitivity

($P > .07$) with the DBT arms that can be attributed to the study design and case selection, where most of the subjects (7684 of 8869) were recruited following a screening mammography recall. However, for invasive tumors of 11–20 mm size, both DBT-FFDM and DBT-SM showed significant improvement ($P < .006$) in sensitivity. With regards to microcalcifications, the AUCs were similar across the three arms, with the sensitivity of DBT-SM being lower than that of DBT-FFDM and FFDM alone.

Most of the aforementioned studies had a case mixture with radiologic

findings of microcalcifications and noncalcified abnormalities. Specific to microcalcifications, an early study (117) observed a nonsignificant improvement in sensitivity and specificity with FFDM compared with DBT. Considering that the study used similar detector technology for FFDM and DBT, detector pixel binning with DBT that reduces spatial resolution or image sharpness, and the longer scan duration with DBT compared with FFDM that increases the likelihood for patient motion, could have contributed to this observation. Independent, retrospective, unblinded

Figure 6

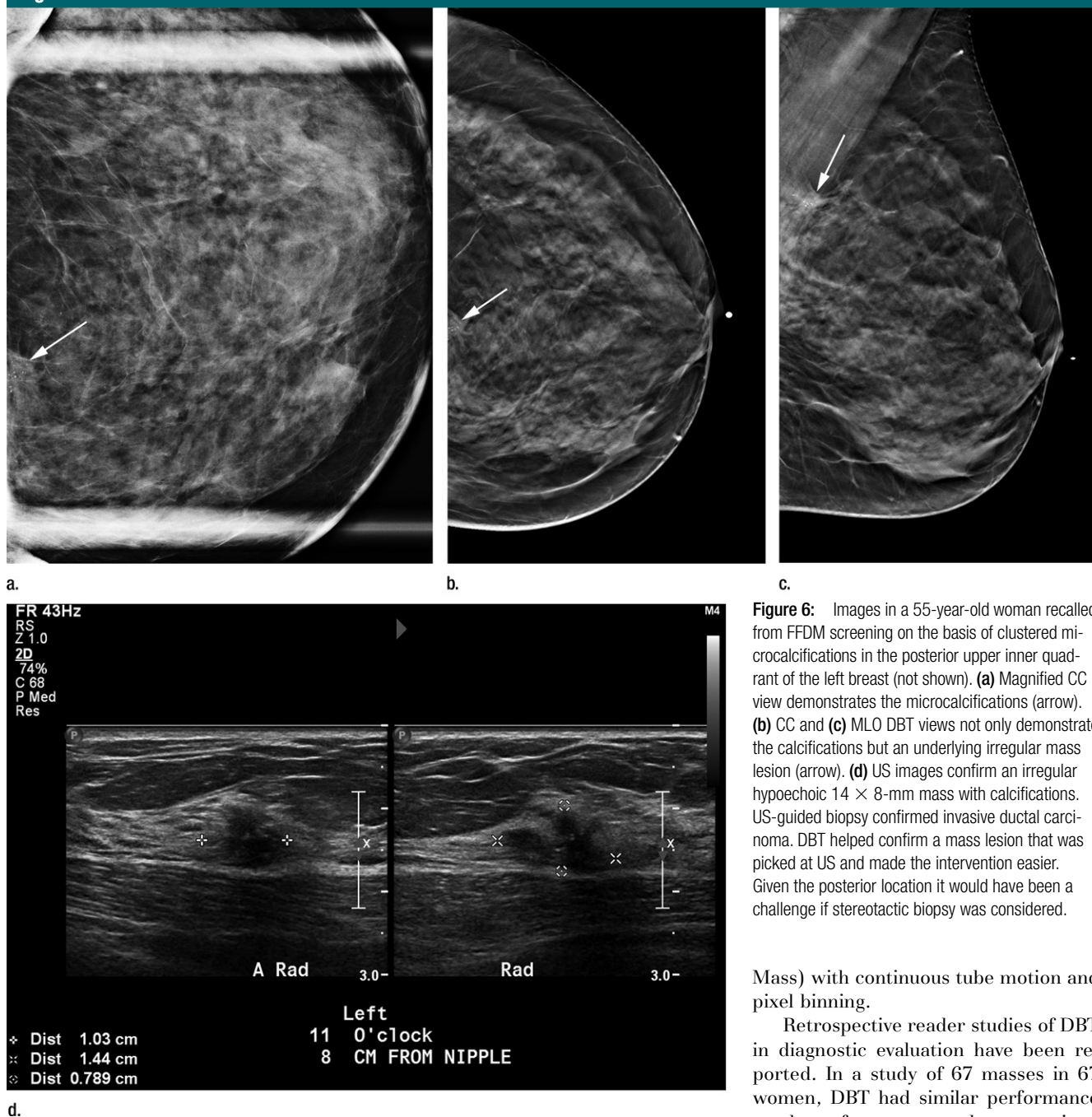


Figure 6: Images in a 55-year-old woman recalled from FFDM screening on the basis of clustered microcalcifications in the posterior upper inner quadrant of the left breast (not shown). **(a)** Magnified CC view demonstrates the microcalcifications (arrow). **(b)** CC and **(c)** MLO DBT views not only demonstrate the calcifications but an underlying irregular mass lesion (arrow). **(d)** US images confirm an irregular hypoechoic 14 × 8-mm mass with calcifications. US-guided biopsy confirmed invasive ductal carcinoma. DBT helped confirm a mass lesion that was picked at US and made the intervention easier. Given the posterior location it would have been a challenge if stereotactic biopsy was considered.

Mass) with continuous tube motion and pixel binning.

Retrospective reader studies of DBT in diagnostic evaluation have been reported. In a study of 67 masses in 67 women, DBT had similar performance to that of mammography spot views (120). In a study of 217 noncalcified lesions in 182 patients that included asymmetries and architectural distortion in addition to masses, the average AUC was higher with DBT than with mammography supplemental views (121). Thibault et al (122) conducted a reader study with 131 breasts from

paired studies (118,119) with 100 or more cases of microcalcifications indicate that approximately 92% of the cases had equal or superior clarity/image quality for visualizing microcalcifications at DBT than at FFDM. The DBT systems used in the two studies

differed; one study (118) used an amorphous silicon-based DBT prototype system (GE Healthcare) with step-and-shoot acquisition and no pixel binning, whereas the other study (119) used an amorphous selenium-based DBT system (Selenia Dimensions; Hologic, Bedford,

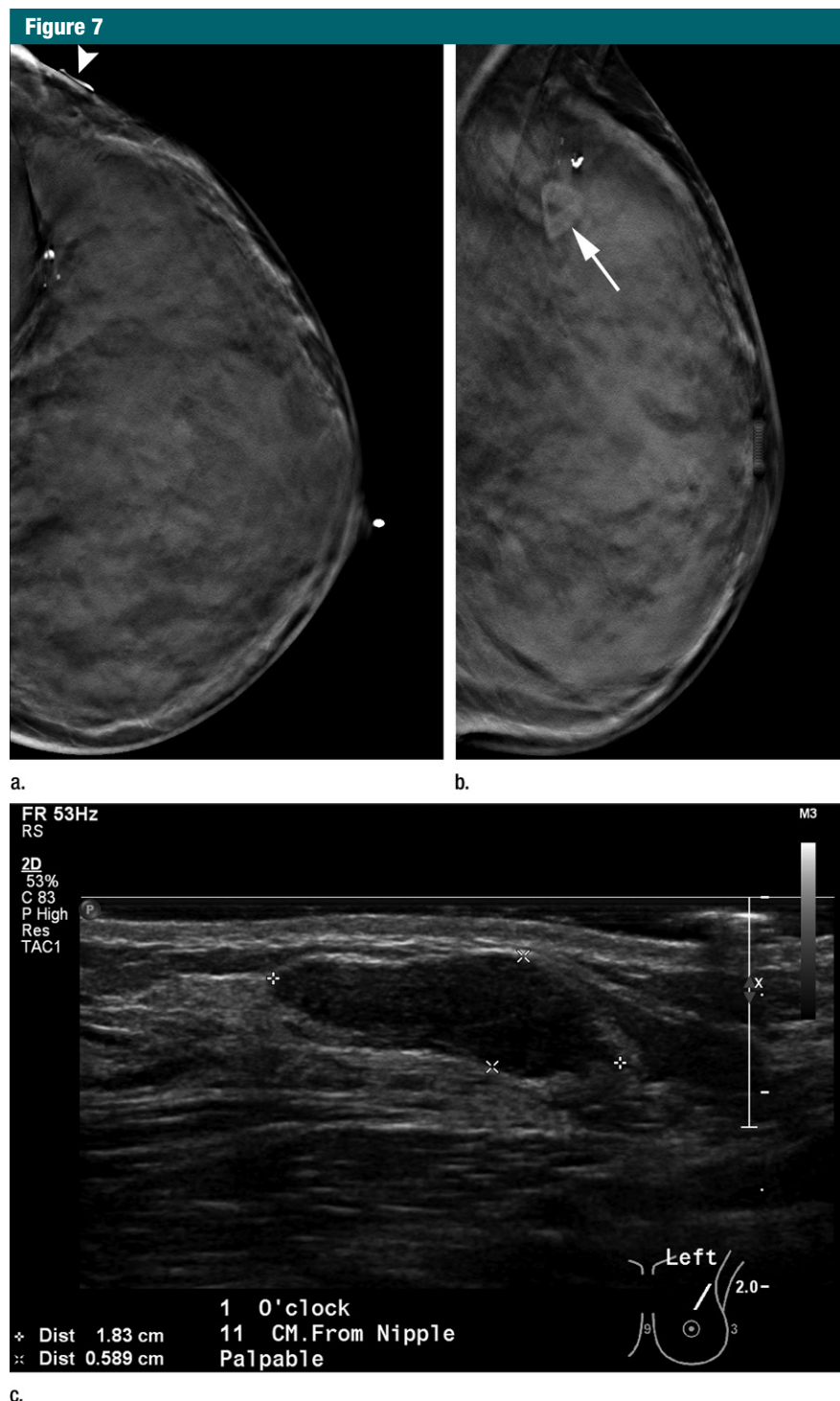


Figure 7: Images in a 41-year-old woman evaluated with diagnostic DBT and FFDM for a palpable lump in the left breast at 1 o'clock. FFDM (not shown) and (a) CC and (b) MLO DBT images demonstrate extremely dense breast and no focal masses were identified. Arrowhead (a) and arrow (b) identify the skin marker corresponding to the location of the palpable lump. However, on (c) US image, a circumscribed mass was noted, and biopsy confirmed fibroadenoma. In extremely dense breasts, DBT images may not demonstrate masses that do not induce desmoplastic reaction.

130 patients who underwent unilateral MLO-view DBT in addition to diagnostic work-up with mammography and US. The study compared mammography alone, mammography with US, DBT alone, combination of DBT and CC-view mammography, and the addition of DBT to mammography and US, and found none of the five tested techniques outperformed in terms of AUC.

A summary of some of the aforementioned studies is provided in Table 3. While the percentage of cases with malignancies are included in the table, a large study (123) investigating abnormality prevalence rates ranging from 2% to 29% in various groups of readers (radiologists, fellows, residents) showed that the “prevalence effect” had negligible contribution in ROC studies. Pilot studies and interim reader studies with less than 100 subjects that preceded some of the studies discussed above have been reported (124–128). Some of the studies used unilateral examinations and the information from contralateral breast was unavailable for comparison. In such studies, it is presumed that the lack of this information has a similar effect on the modalities compared. In most of the studies reviewed above, at least part of the study population underwent DBT on the basis of an abnormal mammogram, constituting a selection bias in favor of mammography. In spite of this bias favoring mammography, retrospective reader studies show either noninferiority or superiority of DBT compared with mammography in terms of AUC or other equivalent figures of merit.

DBT in Clinical Management

The accuracy of tumor size measured with DBT has been reported in several studies. Tumor size of 73 cancers measured by using MLO-view DBT exhibited higher correlation with pathologic findings than FFDM, and was similar to US (129). Applying a criterion of ± 1 cm as threshold for concordance in tumor size with pathologic findings in 173 tumors, Mun et al (130) reported that DBT was more concordant than FFDM. Applying ± 5 mm as threshold for concordance with pathologic findings, Luparia et al

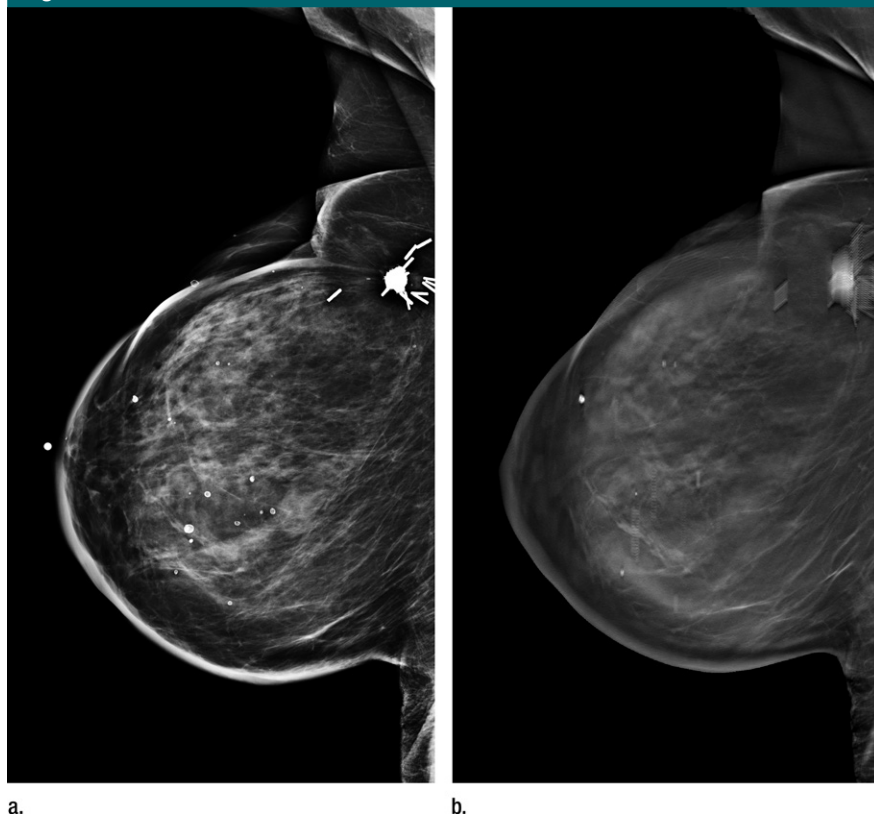
Figure 8

Figure 8: Images in a 71-year-old woman who underwent 1-year follow-up after lumpectomy and radiation therapy with the combined DBT-FFDM examination. **(a)** FFDM image and **(b)** DBT section. DBT section demonstrates artifacts from surgical clips and skin folds.

(131) reported that the concordance and correlation from a study of 149 cancers was highest for MR imaging, followed by DBT, and was better than FFDM and US. A subsequent study (132) of 350 lesions (257 malignancies) reported that compared with MR imaging, the sensitivity and accuracy with the addition of DBT to FFDM and US were similar. Currently, breast MR imaging is the modality of choice for extent of disease evaluation, particularly in patients diagnosed with invasive lobular carcinoma (133). In the aforementioned studies (129–131), invasive lobular carcinoma constituted approximately 4%–21% of lesions. Subanalysis from one study with 31 invasive lobular carcinomas (131) indicated good correlation between pathologic evaluation and DBT, approaching that of MR imaging. However, this is tempered by breast density-dependent

sensitivity of DBT for all malignant lesions and marginally superior performance of MR imaging for multicentric or multifocal disease (132).

Synthesized Digital Mammogram

Synthesis of a digital mammogram from DBT can reduce the radiation dose compared with acquiring both FFDM and DBT images. Currently, at least one vendor has received regulatory approvals. Using an early version of an algorithm for SM, Gur et al (134) conducted a reader study comparing DBT-SM with DBT-FFDM in 114 cases (bilateral two-view examinations), of which 46 cases were malignant (two bilateral malignancies). Compared with DBT-FFDM, a reduction in sensitivity was observed with DBT-SM that was significant for fixed-reader analysis. For 12 of 48 verified cancers and three of the six high-

risk lesions, the images depicted microcalcifications alone. While the recall rate for breasts with no abnormalities or with benign abnormalities did not differ between the two modes, on average 1.6 microcalcification-related abnormalities per reader were missed with DBT-SM. A subsequent reader study (92) using a newer version of the algorithm (C-view; Hologic, Bedford, Mass) used 123 cases, of which 36 were malignant and 48 were benign. The reader-averaged AUCs using probability of malignancy scale and using BIRADS score were not statistically different between DBT-FFDM and DBT-SM. While there was a marginal improvement in AUCs with DBT-FFDM compared with DBT-SM for all eight readers, the differences were smaller than in the study by Gur et al (134) and the differences were not specifically associated with microcalcifications. One arm of the prospective OTST interpreted DBT-SM studies, and a report (91) compared two versions of DBT-SM with DBT-FFDM. With an early version of the SM algorithm applied to DBT from 12631 women in period 1, DBT-SM statistically differed from DBT-FFDM in false-positive rate, whereas with the newer version applied to DBT from 12270 women in period 2, the false-positive rate was not statistically different between DBT-SM and DBT-FFDM. Cancer detection rate showed a nonsignificant decrease with the early version of DBT-SM (period 1) compared with DBT-FFDM. With the newer version, the cancer detection rates with DBT-FFDM (7.8 per 1000) and DBT-SM (7.7 per 1000) were similar. For true-positive scores with verified cancer diagnosis, the number of discordant pairs between DBT-FFDM and DBT-SM was reduced from period 1 and period 2. The above studies show progressive improvement in algorithms used for generating SM. The motivation for including two-dimensional mammograms (either SM or FFDM) is to facilitate easier comparison with prior mammograms to assess temporal changes, and to improve visualization and characterization of microcalcifications. However, the relatively small proportion of findings with microcalcifications alone in the retrospective study (92) and the ob-

Table 3

Enriched Retrospective ROC Studies Comparing DBT and Mammography with a Minimum of 100 Cases

Study and Reference No.	Modalities Compared	No. of Cases	Percentage Malignant	No. of Readers	DBT System*	Key Result
One-View DBT vs Two-View Mammography						
Gennaro et al (111)	MLO-DBT vs two-view FFDM	376 breasts	16.8%	6	General Electric	AUC not different
Wallis et al (34)	MLO-DBT vs two-view FFDM	130 women	30.8%	10	Sectra (Philips)	AUC not different
Svane et al (40)	MLO-DBT vs two-view mammography	144 women	52.7%	2	XCounter	AUC not different
Svahn et al (114)	One-view DBT (88% MLO; 12% CC) vs two-view FFDM	185 breasts	48.1%	5	Siemens	One-view DBT increased AUC†
One-View DBT + One-View FFDM vs Two-View FFDM						
Gennaro et al (112)	MLO-DBT + CC-FFDM vs two-view FFDM	469 breasts	14.5%	6	General Electric	AUC not different‡
Two-View DBT vs Two-View FFDM						
Wallis et al (34)	Two-view DBT vs two-view FFDM	130 women	30.8%	10	Sectra (Philips)	Two-view DBT increased AUC
Two-View DBT + FFDM vs Two-View FFDM						
Rafferty et al (115)	Two-view DBT + FFDM vs two-view FFDM	312 women	15.4%	12	Hologic	Combined two-view DBT + FFDM, increased AUC and reduced false-positive recall rate
Rafferty et al (115)	Two-view DBT + FFDM vs two-view FFDM	310 women	16.5%	15	Hologic	Combined two-view DBT + FFDM, increased AUC and reduced false-positive recall rate
Two-View DBT + FFDM vs Two-View DBT + SM vs Two-View FFDM						
Gilbert et al (116)	Two-view DBT + FFDM vs two-view DBT + SM vs two-view FFDM	7060 women	16.4%	31	Hologic	Two-view DBT + FFDM and two-view DBT + SM increased AUC

Note.—Some studies, particularly those from the same research team, may have partial or complete overlap in dataset. Additional studies are described in the text.

* Some studies used prototype systems that may differ from clinical product.

† Jack-knife free-response ROC analysis (114) also showed a significant increase in figure of merit with one-view DBT compared with two-view FFDM.

‡ Subsequent free-response study (113) showed a statistically significant improvement in lesion detection and lesion characterization fractions with MLO-DBT plus CC-FFDM versus two-view FFDM.

servation that some false-positive scores were assigned to benign microcalcifications in the prospective trial (91) suggest the need for further studies. Also, the effect of pixel binning during DBT acquisition on the generated SM needs to be investigated. It may also be possible to apply CAD to SM, which to our knowledge has not been reported.

Interpretation Time

An early study noted that the average interpretation times for DBT reconstructions were substantially higher than for FFDM (124). A subsequent study also observed that the average interpretation time for the combined DBT-FFDM study was substantially higher than for FFDM (109). A more recent study suggested that extensive training of radiologists alone may not be sufficient to

reduce interpretation time from DBT-FFDM studies to that of FFDM studies (135). In all of the aforementioned studies on interpretation time, there were multiple rating scales or extensive reporting for study purposes that were included in the interpretation time, and these studies would not be representative of standard clinical practice. In the prospective OTST trial (95), it was reported that the interpretation time was 91 seconds for the DBT-FFDM studies and was significantly higher than for FFDM alone (45 seconds). In another prospective study (136), 10 radiologists with varying breast imaging experience (1.5–21 years) batch read 1502 combined DBT-FFDM studies and 2163 FFDM studies in a manner replicative of normal clinical workflow. It was reported that the average interpretation

time for the DBT-FFDM studies was 2.8 minutes compared with 1.9 minutes for FFDM alone. The study noted that the additional interpretation time with the DBT-FFDM study decreased with increased radiologist experience. However, with the exception of one radiologist, all radiologists increased their interpretation time with DBT-FFDM. While DBT-FFDM may provide for reduced recall rate thereby reducing the time and resources for diagnostic evaluation, the increased interpretation time with DBT-FFDM needs to be considered for resource and workflow management.

Advanced Applications

The advent of DBT has prompted investigations into the development of CAD for DBT. Studies applying CAD to 2D

DBT projections (137,138), DBT reconstructions (138–141), and the combination of 2D projections and reconstructions (138,142) for detection of masses have been reported. For detection of microcalcifications, CAD applied to 2D projections (143) and DBT reconstructions (144,145) have been reported. Considering that several studies show an improvement in detection of soft-tissue abnormalities with DBT, CAD applied for detection of microcalcifications is likely to be more important. Among the studies investigating CAD for microcalcifications, one study with two-view DBT of 154 breasts (116 with microcalcifications) observed that on a per-breast basis, sensitivity was 85% at a false-positive rate of 0.85 per breast (145). Considering that the field is gravitating toward a combination of DBT and 2D mammography (either SM or FFDM), the benefit of applying CAD to DBT versus CAD to 2D mammography that is widely used is unclear and needs investigation.

The clinical availability of DBT also necessitates the development of biopsy guidance devices compatible with DBT. Several DBT system manufacturers have already developed or are developing such biopsy attachments (146,147).

A preliminary study of contrast-media-enhanced DBT (148) with 13 subjects demonstrated feasibility of using single-energy temporal subtraction technique. A subsequent study (149) demonstrated the feasibility of dual-energy technique, where DBT images were acquired at multiple time points after contrast agent administration and could facilitate analysis of contrast agent kinetics. Temporal subtraction techniques may require additional image processing to alleviate patient motion artifacts. Using a photon-counting DBT system that facilitates simultaneous acquisition of low- and high-energy images, Schmitzberger et al (150) demonstrated feasibility of contrast-media-enhanced DBT. Further studies are needed to address diagnostic benefit of contrast-media-enhanced DBT.

Multimodality Imaging

The development of multimodality systems combining DBT with automated US, radionuclide imaging, or near-in-

frared imaging is being actively pursued. An initial study (151) combined FFDM with three-dimensional automated breast US enabling coregistered dual-modality imaging and was subsequently modified for DBT with automated breast US. Development of a compression paddle compatible for both x-ray and US imaging (152), selection of US coupling media, and breast coverage with US particularly at the breast periphery that is not in contact with the compression paddle have been reported (153). In an analysis of 51 patients with masses (13 malignancies), Padilla et al (154) reported similar AUCs for DBT alone and the combined DBT and automated breast US, and an improvement in discriminating masses from simple cysts.

A dual-modality system combining DBT with compact gamma camera (155) was used to image 17 women with 21 lesions (seven malignancies) after administration of technetium 99m, demonstrating the feasibility of coregistered anatomic and functional images (156). Multiple research teams are investigating the combination of DBT with near-infrared spectroscopy, or NIRS (157–160). NIRS can estimate hemoglobin concentration and oxygen saturation, which have the potential to discriminate between benign and malignant lesions. While the spatial resolution of NIRS alone is poor, spatial distribution of anatomy from DBT can be incorporated during NIRS reconstruction to substantially improve spatial resolution. In a study of 189 breasts from 125 women, including 51 breasts with lesions (26 malignancies), hemoglobin concentrations for malignancies were significantly higher than the fibroglandular tissue of the same breast, and malignancies could be distinguished from benign lesions and cysts (158). All of these multimodality systems are in the investigational phase and may take several years of research before translating to clinical use.

Summary

Almost all studies reported to date with DBT alone or a combination of DBT

with FFDM show that DBT is either noninferior or superior to FFDM, with the exception of an early study on microcalcifications (117). While studies (40,111) comparing one-view DBT with two-view FFDM demonstrated noninferiority of one-view DBT, and one study (114) showed superiority of one-view DBT, the study (34) comparing two-view and one-view DBT with FFDM observed superiority of two-view DBT over FFDM. This suggests two-view DBT would be preferable. Studies that included at least one-view FFDM with DBT have shown improvement over two-view FFDM (113,115,126). Progressive improvements (91,92) with newer versions of algorithms for generating SM suggest that it may be a potential approach for limiting radiation dose and needs further investigation (28). All of the aforementioned observations have to be qualified in that the results from the discussed studies may only be applicable for specific DBT systems and may not be generalized across DBT systems from multiple vendors that vary in design, technological implementation, and reconstruction algorithms. At present, clinical studies with DBT systems from multiple vendors are lacking. It is important to recognize that if DBT is performed on the basis of an abnormal screening mammogram, then the sensitivity of DBT cannot exceed that of mammography. The OTST and STORM trials (95,96) showed the value of DBT as a screening tool. To increase cancer detection rate, women need to undergo DBT as part of their screening. While DBT may provide a substantial benefit over FFDM, there may be instances when an abnormality is occult (161). Transition to DBT should consider economic and logistic factors (162), such as the increase in interpretation time (135,136) and cost-effectiveness (163). At the institutional level, compatibility of DBT with existing picture archiving and communication systems and with the review workstation used for interpretation need to be considered. A clinical study on the relative merits of DBT and automated breast US in screening women with radiographically dense breasts needs investigation.

Disclosure: At the time of this writing, some of the DBT systems discussed in the article have not received U.S. Food and Drug Administration approval.

Disclosures of Conflicts of Interest: **S.V.** Activities related to the present article: none to disclose. Activities not related to the present article: grant from Koning Corporation (West Henrietta, NY). Other relationships: issued patent US 8817947 B2 held by University of Massachusetts Medical School. **A.K.** Activities related to the present article: none to disclose. Activities not related to the present article: grant from Koning Corporation. Other relationships: issued patent US 8817947 B2 held by University of Massachusetts Medical School. **G.R.V.** Activities related to the present article: none to disclose. Activities not related to the present article: grant from Koning Corporation. Other relationships: none to disclose. **D.B.K.** Activities related to the present article: has received grants from General Electric, the Department of the Army, Siemens, and Hologic. Activities not related to the present article: General Electric has licensed the patent on digital breast tomosynthesis held by Massachusetts General Hospital (US 5872828 A). Other relationships: none to disclose.

References

1. Tabar L, Fagerberg G, Chen HH, et al. Efficacy of breast cancer screening by age: new results from the Swedish Two-County Trial. *Cancer* 1995;75(10):2507–2517.
2. Nyström L, Andersson I, Bjurström N, Frisell J, Nordenskjöld B, Rutqvist LE. Long-term effects of mammography screening: updated overview of the Swedish randomised trials. *Lancet* 2002;359(9310):909–919.
3. Berry DA, Cronin KA, Plevritis SK, et al. Effect of screening and adjuvant therapy on mortality from breast cancer. *N Engl J Med* 2005;353(17):1784–1792.
4. Swedish Organised Service Screening Evaluation Group. Reduction in breast cancer mortality from organized service screening with mammography: 1. Further confirmation with extended data. *Cancer Epidemiol Biomarkers Prev* 2006;15(1):45–51.
5. Swedish Organised Service Screening Evaluation Group. Reduction in breast cancer mortality from the organized service screening with mammography: 2. Validation with alternative analytic methods. *Cancer Epidemiol Biomarkers Prev* 2006;15(1):52–56.
6. Kerlikowske K, Grady D, Barclay J, Sickles EA, Ernster V. Effect of age, breast density, and family history on the sensitivity of first screening mammography. *JAMA* 1996;276(1):33–38.
7. Rosenberg RD, Hunt WC, Williamson MR, et al. Effects of age, breast density, ethnicity, and estrogen replacement therapy on screening mammographic sensitivity and cancer stage at diagnosis: review of 183,134 screening mammograms in Albuquerque, New Mexico. *Radiology* 1998;209(2):511–518.
8. Kolb TM, Lichy J, Newhouse JH. Comparison of the performance of screening mammography, physical examination, and breast US and evaluation of factors that influence them: an analysis of 27,825 patient evaluations. *Radiology* 2002;225(1):165–175.
9. Sickles EA, Miglioretti DL, Ballard-Barbash R, et al. Performance benchmarks for diagnostic mammography. *Radiology* 2005;235(3):775–790.
10. Rowlands JA, Hunter DM, Araj N. X-ray imaging using amorphous selenium: a photo-induced discharge readout method for digital mammography. *Med Phys* 1991;18(3):421–431.
11. Vedantham S, Karellas A, Suryanarayanan S, et al. Full breast digital mammography with an amorphous silicon-based flat panel detector: physical characteristics of a clinical prototype. *Med Phys* 2000;27(3):558–567.
12. Ren B, Ruth C, Stein J, Smith A, Shaw I, Jing Z. Design and performance of the prototype full field breast tomosynthesis system with selenium based flat panel detector. In: Flynn MJ, ed. *Proceedings of SPIE: medical imaging 2005—physics of medical imaging*. Vol 5745. Bellingham, Wash: International Society for Optics and Photonics, 2005; 550–561.
13. Pisano ED, Gatsonis C, Hendrick E, et al. Diagnostic performance of digital versus film mammography for breast-cancer screening. *N Engl J Med* 2005;353(17):1773–1783.
14. Elmore JG, Jackson SL, Abraham L, et al. Variability in interpretive performance at screening mammography and radiologists' characteristics associated with accuracy. *Radiology* 2009;253(3):641–651.
15. Burgess AE, Jacobson FL, Judy PF. Human observer detection experiments with mammograms and power-law noise. *Med Phys* 2001;28(4):419–437.
16. Niklason LT, Christian BT, Niklason LE, et al. Digital tomosynthesis in breast imaging. *Radiology* 1997;205(2):399–406.
17. Ziedses des Plantes BG. Eine Neue Methode Zur Differenzierung in der Röntgenographie (Planigraphie). *Acta Radiol* 1932;13(2):182–192.
18. Niklason LT, Niklason LE, Kopans DB, inventors; the General Hospital Corp, original assignee. Tomosynthesis system for breast imaging. USPTO 5872828 A. February 16, 1999.
19. Dobbins JT 3rd, Godfrey DJ. Digital x-ray tomosynthesis: current state of the art and clinical potential. *Phys Med Biol* 2003;48(19):R65–R106.
20. Karellas A, Vedantham S. Breast cancer imaging: a perspective for the next decade. *Med Phys* 2008;35(11):4878–4897.
21. Skaane P. Studies comparing screen-film mammography and full-field digital mammography in breast cancer screening: updated review. *Acta Radiol* 2009;50(1):3–14.
22. Helvie MA. Digital mammography imaging: breast tomosynthesis and advanced applications. *Radiol Clin North Am* 2010;48(5):917–929.
23. D'Orsi CJ, Newell MS. On the frontline of screening for breast cancer. *Semin Oncol* 2011;38(1):119–127.
24. Park JM, Franken EA Jr, Garg M, Fajardo LL, Niklason LT. Breast tomosynthesis: present considerations and future applications. *RadioGraphics* 2007;27(Suppl 1):S231–S240.
25. Baker JA, Lo JY. Breast tomosynthesis: state-of-the-art and review of the literature. *Acad Radiol* 2011;18(10):1298–1310.
26. Diekmann F, Bick U. Breast tomosynthesis. *Semin Ultrasound CT MR* 2011;32(4):281–287.
27. Alakhras M, Bourne R, Rickard M, Ng KH, Pietrzyk M, Brennan PC. Digital tomosynthesis: a new future for breast imaging? *Clin Radiol* 2013;68(5):e225–e236.
28. Houssami N, Skaane P. Overview of the evidence on digital breast tomosynthesis in breast cancer detection. *Breast* 2013;22(2):101–108.
29. Uematsu T. The emerging role of breast tomosynthesis. *Breast Cancer* 2013;20(3):204–212.
30. Sechopoulos I. A review of breast tomosynthesis. Part I. The image acquisition process. *Med Phys* 2013;40(1):014301.
31. Sechopoulos I. A review of breast tomosynthesis. Part II. Image reconstruction, processing and analysis, and advanced applications. *Med Phys* 2013;40(1):014302.
32. Kopans DB. Digital breast tomosynthesis from concept to clinical care. *AJR Am J Roentgenol* 2014;202(2):299–308.
33. van Engen R, Bosmans H, Bouwman R, et al. EUREF Draft QC protocol for breast tomosynthesis systems. Version 0.15. <http://www.euref.org/downloads?download=47:euref-tomo-protocol-version-015>. Published January 2014.

34. Wallis MG, Moa E, Zanca F, Leifland K, Danielsson M. Two-view and single-view tomosynthesis versus full-field digital mammography: high-resolution x-ray imaging observer study. *Radiology* 2012;262(3):788–796.
35. Mainprize JG, Bloomquist AK, Kempston MP, Yaffe MJ. Resolution at oblique incidence angles of a flat panel imager for breast tomosynthesis. *Med Phys* 2006;33(9):3159–3164.
36. Badano A, Kyprianou IS, Jennings RJ, Sempau J. Anisotropic imaging performance in breast tomosynthesis. *Med Phys* 2007;34(11):4076–4091.
37. Que W, Rowlands JA. X-ray imaging using amorphous selenium: inherent spatial resolution. *Med Phys* 1995;22(4):365–374.
38. Badano A, Freed M, Fang Y. Oblique incidence effects in direct x-ray detectors: a first-order approximation using a physics-based analytical model. *Med Phys* 2011;38(4):2095–2098.
39. Freed M, Park S, Badano A. A fast, angle-dependent, analytical model of CsI detector response for optimization of 3D x-ray breast imaging systems. *Med Phys* 2010;37(6):2593–2605.
40. Svane G, Azavedo E, Lindman K, et al. Clinical experience of photon counting breast tomosynthesis: comparison with traditional mammography. *Acta Radiol* 2011;52(2):134–142.
41. Mainprize JG, Bloomquist A, Wang X, Yaffe MJ. Dependence of image quality on geometric factors in breast tomosynthesis. *Med Phys* 2011;38(6):3090–3103.
42. Hu YH, Zhao B, Zhao W. Image artifacts in digital breast tomosynthesis: investigation of the effects of system geometry and reconstruction parameters using a linear system approach. *Med Phys* 2008;35(12):5242–5252.
43. Sechopoulos I, Ghetti C. Optimization of the acquisition geometry in digital tomosynthesis of the breast. *Med Phys* 2009;36(4):1199–1207.
44. Bissonnette M, Hansroul M, Masson E, et al. Digital breast tomosynthesis using an amorphous selenium flat panel detector. In: Flynn MJ, ed. *Proceedings of SPIE: medical imaging 2005—physics of medical imaging*. Vol 5745. Bellingham, Wash: International Society for Optics and Photonics, 2005; 529–540.
45. Cheung LK, Jing Z, Bogdanovich S, et al. Image performance of a new amorphous selenium flat panel x-ray detector designed for digital breast tomosynthesis. In: Flynn MJ, ed. *Proceedings of SPIE: medical imaging 2005—physics of medical imaging*. Vol 5745. Bellingham, Wash: International Society for Optics and Photonics, 2005; 1282–1290.
46. Eberhard JW, Staudinger P, Smolenski J, et al. High-speed large angle mammography tomosynthesis system. In: Flynn MJ, Hsieh J, eds. *Proceedings of SPIE: medical imaging 2006—physics of medical imaging*. Vol 6142. Bellingham, Wash: International Society for Optics and Photonics, 2006; 61420C.
47. Zhao W, Zhao B, Fisher PR, Warmoes P, Mertelmeier T, Orman J. Optimization of detector operation and imaging geometry for breast tomosynthesis. In: Hsieh J, Flynn MJ, eds. *Proceedings of SPIE: medical imaging 2007—physics of medical imaging*. Vol 6510. Bellingham, Wash: International Society for Optics and Photonics, 2007; 65101M.
48. Zhao B, Zhao W. Imaging performance of an amorphous selenium digital mammography detector in a breast tomosynthesis system. *Med Phys* 2008;35(5):1978–1987.
49. Okada Y, Sato K, Ito T, Hosoi Y, Hayakawa T. A newly developed a-Se mammography flat panel detector with high-sensitivity and low image artifact. In: Nishikawa RM, Whiting BR, Hoeschen C, eds. *Proceedings of SPIE: medical imaging 2013—physics of medical imaging*. Vol 8668. Bellingham, Wash: International Society for Optics and Photonics, 2013; 86685V.
50. Schulze-Hagen M, Eshghi N, Muller J, Muller-Leisse C. Efficacy of tomosynthesis (DBT) in respect to two different modes (HR vs ST) in a clinical setting. Preliminary results. *European Congress of Radiology*. Vienna, Austria: European Society of Radiology, 2014; Poster No. C-1139.
51. Suryanarayanan S, Karellas A, Vedantham S, et al. Comparison of tomosynthesis methods used with digital mammography. *Acad Radiol* 2000;7(12):1085–1097.
52. Suryanarayanan S, Karellas A, Vedantham S, et al. Evaluation of linear and nonlinear tomographic reconstruction methods in digital mammography. *Acad Radiol* 2001;8(3):219–224.
53. Webber RL, Horton RA, Tyndall DA, Ludlow JB. Tuned-aperture computed tomography (TACT). Theory and application for three-dimensional dento-alveolar imaging. *Dentomaxillofac Radiol* 1997;26(1):53–62.
54. Ruttimann UE, Groenhuis RA, Webber RL. Restoration of digital multiplane tomosynthesis by a constrained iteration method. *IEEE Trans Med Imaging* 1984;3(3):141–148.
55. Wu T, Moore RH, Rafferty EA, Kopans DB. A comparison of reconstruction algorithms for breast tomosynthesis. *Med Phys* 2004;31(9):2636–2647.
56. Chen Y, Lo JY, Dobbins JT 3rd. Importance of point-by-point back projection correction for isocentric motion in digital breast tomosynthesis: relevance to morphology of structures such as microcalcifications. *Med Phys* 2007;34(10):3885–3892.
57. Zhou J, Zhao B, Zhao W. A computer simulation platform for the optimization of a breast tomosynthesis system. *Med Phys* 2007;34(3):1098–1109.
58. Zhao B, Zhao W. Three-dimensional linear system analysis for breast tomosynthesis. *Med Phys* 2008;35(12):5219–5232.
59. Zhao B, Zhou J, Hu YH, Mertelmeier T, Ludwig J, Zhao W. Experimental validation of a three-dimensional linear system model for breast tomosynthesis. *Med Phys* 2009;36(1):240–251.
60. Mertelmeier T, Orman J, Haerer W, Duda MK. Optimizing filtered backprojection reconstruction for a breast tomosynthesis prototype device. In: Flynn MJ, Hsieh J, eds. *Proceedings of SPIE: medical imaging 2006—physics of medical imaging*. Vol 6142. Bellingham, Wash: International Society for Optics and Photonics, 2006; 61420F.
61. Orman J, Mertelmeier T, Haerer W. Adaptation of image quality using various filter setups in the filtered back-projection approach for digital breast tomosynthesis. *Lect Notes Comput Sci* 2006;4046:175–182.
62. Claus BE, Eberhard JW, Schmitz A, Carson P, Goodsitt M, Chan HP. Generalized filtered back-projection reconstruction in breast tomosynthesis. *Lect Notes Comput Sci* 2006;4046:167–174.
63. Zhang Y, Chan HP, Sahiner B, et al. A comparative study of limited-angle cone-beam reconstruction methods for breast tomosynthesis. *Med Phys* 2006;33(10):3781–3795.
64. Lu Y, Chan HP, Wei J, Hadjiiski LM. Selective-diffusion regularization for enhancement of microcalcifications in digital breast tomosynthesis reconstruction. *Med Phys* 2010;37(11):6003–6014.
65. Chen Y, Lo JY, Baker JA, Dobbins JT Jr. Gaussian frequency blending algorithm with matrix inversion tomosynthesis (MITS) and filtered back projection (FBP) for better digital breast tomosynthesis reconstruction. In: Flynn MJ, Hsieh J, eds. *Proceedings of SPIE: medical imaging 2006—physics of medical imaging*. Vol 6142.

- Bellingham, Wash: International Society for Optics and Photonics, 2006; 61420E.
66. Sidky EY, Pan X, Reiser IS, Nishikawa RM, Moore RH, Kopans DB. Enhanced imaging of microcalcifications in digital breast tomosynthesis through improved image-reconstruction algorithms. *Med Phys* 2009; 36(11):4920–4932.
 67. Chung J, Nagy JG, Sechopoulos I. Numerical algorithms for polyenergetic digital breast tomosynthesis reconstruction. *SIAM J Imaging Sci* 2010;3(1):133–152.
 68. Das M, Gifford HC, O'Connor JM, Glick SJ. Penalized maximum likelihood reconstruction for improved microcalcification detection in breast tomosynthesis. *IEEE Trans Med Imaging* 2011;30(4):904–914.
 69. Van de Sompel D, Brady M. Regularising limited view tomography using anatomical reference images and information theoretic similarity metrics. *Med Image Anal* 2012;16(1):278–300.
 70. Hammerstein GR, Miller DW, White DR, Masterson ME, Woodard HQ, Laughlin JS. Absorbed radiation dose in mammography. *Radiology* 1979;130(2):485–491.
 71. Sechopoulos I, Suryanarayanan S, Vedantham S, D'Orsi C, Karellas A. Computation of the glandular radiation dose in digital tomosynthesis of the breast. *Med Phys* 2007;34(1):221–232.
 72. Ma AK, Darambara DG, Stewart A, Gunn S, Bullard E. Mean glandular dose estimation using MCNPX for a digital breast tomosynthesis system with tungsten/aluminum and tungsten/aluminum+silver x-ray anode-filter combinations. *Med Phys* 2008;35(12):5278–5289.
 73. Sechopoulos I, D'Orsi CJ. Glandular radiation dose in tomosynthesis of the breast using tungsten targets. *J Appl Clin Med Phys* 2008;9(4):2887.
 74. Myronakis ME, Zvelebil M, Darambara DG. Normalized mean glandular dose computation from mammography using GATE: a validation study. *Phys Med Biol* 2013; 58(7):2247–2265.
 75. Vedantham S, Shi L, Karellas A, O'Connell AM, Conover DL. Personalized estimates of radiation dose from dedicated breast CT in a diagnostic population and comparison with diagnostic mammography. *Phys Med Biol* 2013;58(22):7921–7936.
 76. Dance DR, Young KC, van Engen RE. Estimation of mean glandular dose for breast tomosynthesis: factors for use with the UK, European and IAEA breast dosimetry protocols. *Phys Med Biol* 2011;56(2):453–471.
 77. Sechopoulos I, Sabol JM, Berglund J, et al. Radiation dosimetry in digital breast tomosynthesis: report of AAPM Tomosynthesis Subcommittee Task Group 223. *Med Phys* 2014;41(9):091501.
 78. Feng SS, Sechopoulos I. Clinical digital breast tomosynthesis system: dosimetric characterization. *Radiology* 2012;263(1):35–42.
 79. Yaffe MJ, Boone JM, Packard N, et al. The myth of the 50-50 breast. *Med Phys* 2009; 36(12):5437–5443.
 80. Nelson TR, Cerviño LI, Boone JM, Lindfors KK. Classification of breast computed tomography data. *Med Phys* 2008;35(3):1078–1086.
 81. Vedantham S, Shi L, Karellas A, O'Connell AM. Dedicated breast CT: fibroglandular volume measurements in a diagnostic population. *Med Phys* 2012;39(12):7317–7328.
 82. Chang DH, Chen JH, Lin M, et al. Comparison of breast density measured on MR images acquired using fat-suppressed versus nonfat-suppressed sequences. *Med Phys* 2011;38(11):5961–5968.
 83. Olgar T, Kahn T, Gosch D. Average glandular dose in digital mammography and breast tomosynthesis. *Rofo* 2012; 184(10):911–918.
 84. Cavagnetto F, Taccini G, Rosasco R, Bampi R, Calabrese M, Tagliafico A. 'In vivo' average glandular dose evaluation: one-to-one comparison between digital breast tomosynthesis and full-field digital mammography. *Radiat Prot Dosimetry* 2013;157(1):53–61.
 85. Bernardi D, Caumo F, Macaskill P, et al. Effect of integrating 3D-mammography (digital breast tomosynthesis) with 2D-mammography on radiologists' true-positive and false-positive detection in a population breast screening trial. *Eur J Cancer* 2014;50(7):1232–1238.
 86. Skaane P, Bandos AI, Gullien R, et al. Prospective trial comparing full-field digital mammography (FFDM) versus combined FFDM and tomosynthesis in a population-based screening programme using independent double reading with arbitration. *Eur Radiol* 2013;23(8):2061–2071.
 87. Teertstra HJ, Loo CE, van den Bosch MA, et al. Breast tomosynthesis in clinical practice: initial results. *Eur Radiol* 2010;20(1):16–24.
 88. Hendrick RE, Pisano ED, Averbukh A, et al. Comparison of acquisition parameters and breast dose in digital mammography and screen-film mammography in the American College of Radiology Imaging Network digital mammographic imaging screening trial. *AJR Am J Roentgenol* 2010;194(2):362–369.
 89. Hendrick RE. Radiation doses and cancer risks from breast imaging studies. *Radiology* 2010;257(1):246–253.
 90. Svahn TM, Houssami N, Sechopoulos I, Mattsson S. Review of radiation dose estimates in digital breast tomosynthesis relative to those in two-view full-field digital mammography. *Breast* 2015;24(2):93–99.
 91. Skaane P, Bandos AI, Eben EB, et al. Two-view digital breast tomosynthesis screening with synthetically reconstructed projection images: comparison with digital breast tomosynthesis with full-field digital mammographic images. *Radiology* 2014;271(3):655–663.
 92. Zuley ML, Guo B, Catullo VJ, et al. Comparison of two-dimensional synthesized mammograms versus original digital mammograms alone and in combination with tomosynthesis images. *Radiology* 2014; 271(3):664–671.
 93. Nishikawa RM, Reiser I, Seifi P, Vyborny CJ. A new approach to digital breast tomosynthesis for breast cancer screening. In: Hsieh J, Flynn MJ, eds. *Proceedings of SPIE: medical imaging 2007—physics of medical imaging*. Vol 6510. Bellingham, Wash: International Society for Optics and Photonics, 2007; 65103C.
 94. Vecchio S, Albanese A, Vignoli P, Taibi A. A novel approach to digital breast tomosynthesis for simultaneous acquisition of 2D and 3D images. *Eur Radiol* 2011;21(6):1207–1213.
 95. Skaane P, Bandos AI, Gullien R, et al. Comparison of digital mammography alone and digital mammography plus tomosynthesis in a population-based screening program. *Radiology* 2013;267(1):47–56.
 96. Ciatto S, Houssami N, Bernardi D, et al. Integration of 3D digital mammography with tomosynthesis for population breast-cancer screening (STORM): a prospective comparison study. *Lancet Oncol* 2013;14(7):583–589.
 97. Caumo F, Bernardi D, Ciatto S, et al. Incremental effect from integrating 3D-mammography (tomosynthesis) with 2D-mammography: Increased breast cancer detection evident for screening centres in a population-based trial. *Breast* 2014;23(1):76–80.
 98. Rose SL, Tidwell AL, Bujnoch LJ, Kushwaha AC, Nordmann AS, Sexton R Jr. Implementation of breast tomosynthesis in a routine screening practice: an observational

- study. *AJR Am J Roentgenol* 2013;200(6):1401–1408.
99. McCarthy AM, Kontos D, Synnestvedt M, et al. Screening outcomes following implementation of digital breast tomosynthesis in a general-population screening program. *J Natl Cancer Inst* 2014;106(11):dju316.
 100. Durand MA, Haas BM, Yao X, et al. Early clinical experience with digital breast tomosynthesis for screening mammography. *Radiology* 2015;274(1):85–92.
 101. Haas BM, Kalra V, Geisel J, Raghu M, Durand M, Philpotts LE. Comparison of tomosynthesis plus digital mammography and digital mammography alone for breast cancer screening. *Radiology* 2013;269(3):694–700.
 102. Friedewald SM, Rafferty EA, Rose SL, et al. Breast cancer screening using tomosynthesis in combination with digital mammography. *JAMA* 2014;311(24):2499–2507.
 103. Lång K, Andersson I, Rosso A, Tingberg A, Timberg P, Zackrisson S. Performance of one-view breast tomosynthesis as a stand-alone breast cancer screening modality: results from the Malmö Breast Tomosynthesis Screening Trial, a population-based study. *Eur Radiol* 2015.
 104. Michell MJ, Iqbal A, Wasan RK, et al. A comparison of the accuracy of film-screen mammography, full-field digital mammography, and digital breast tomosynthesis. *Clin Radiol* 2012;67(10):976–981.
 105. Poplack SP, Tosteson TD, Kogel CA, Nagy HM. Digital breast tomosynthesis: initial experience in 98 women with abnormal digital screening mammography. *AJR Am J Roentgenol* 2007;189(3):616–623.
 106. Skaane P, Gullien R, Bjørndal H, et al. Digital breast tomosynthesis (DBT): initial experience in a clinical setting. *Acta Radiol* 2012;53(5):524–529.
 107. Waldherr C, Cerny P, Altermatt HJ, et al. Value of one-view breast tomosynthesis versus two-view mammography in diagnostic workup of women with clinical signs and symptoms and in women recalled from screening. *AJR Am J Roentgenol* 2013;200(1):226–231.
 108. Brandt KR, Craig DA, Hoskins TL, et al. Can digital breast tomosynthesis replace conventional diagnostic mammography views for screening recalls without calcifications? A comparison study in a simulated clinical setting. *AJR Am J Roentgenol* 2013;200(2):291–298.
 109. Gur D, Abrams GS, Chough DM, et al. Digital breast tomosynthesis: observer performance study. *AJR Am J Roentgenol* 2009;193(2):586–591.
 110. Gur D, Bandos AI, Rockette HE, et al. Localized detection and classification of abnormalities on FFDM and tomosynthesis examinations rated under an FROC paradigm. *AJR Am J Roentgenol* 2011;196(3):737–741.
 111. Gennaro G, Toledano A, di Maggio C, et al. Digital breast tomosynthesis versus digital mammography: a clinical performance study. *Eur Radiol* 2010;20(7):1545–1553.
 112. Gennaro G, Hendrick RE, Ruppel P, et al. Performance comparison of single-view digital breast tomosynthesis plus single-view digital mammography with two-view digital mammography. *Eur Radiol* 2013;23(3):664–672.
 113. Gennaro G, Hendrick RE, Toledano A, et al. Combination of one-view digital breast tomosynthesis with one-view digital mammography versus standard two-view digital mammography: per lesion analysis. *Eur Radiol* 2013;23(8):2087–2094.
 114. Svahn TM, Chakraborty DP, Ikeda D, et al. Breast tomosynthesis and digital mammography: a comparison of diagnostic accuracy. *Br J Radiol* 2012;85(1019):e1074–e1082.
 115. Rafferty EA, Park JM, Philpotts LE, et al. Assessing radiologist performance using combined digital mammography and breast tomosynthesis compared with digital mammography alone: results of a multicenter, multireader trial. *Radiology* 2013;266(1):104–113.
 116. Gilbert FJ, Tucker L, Gillan MG, et al. The TOMMY trial: a comparison of TOMosynthesis with digital MammographY in the UK NHS Breast Screening Programme—a multicentre retrospective reading study comparing the diagnostic performance of digital breast tomosynthesis and digital mammography with digital mammography alone. *Health Technol Assess* 2015;19(4):i–xxv, 1–136.
 117. Spangler ML, Zuley ML, Sumkin JH, et al. Detection and classification of calcifications on digital breast tomosynthesis and 2D digital mammography: a comparison. *AJR Am J Roentgenol* 2011;196(2):320–324.
 118. Kopans D, Gavenonis S, Halpern E, Moore R. Calcifications in the breast and digital breast tomosynthesis. *Breast J* 2011;17(6):638–644.
 119. Destounis SV, Arieno AL, Morgan RC. Preliminary clinical experience with digital breast tomosynthesis in the visualization of breast microcalcifications. *J Clin Imaging Sci* 2013;3:65.
 120. Noroozian M, Hadjiiski L, Rahnema-Moghadam S, et al. Digital breast tomosynthesis is comparable to mammographic spot views for mass characterization. *Radiology* 2012;262(1):61–68.
 121. Zuley ML, Bandos AI, Ganott MA, et al. Digital breast tomosynthesis versus supplemental diagnostic mammographic views for evaluation of noncalcified breast lesions. *Radiology* 2013;266(1):89–95.
 122. Thibault F, Dromain C, Breucq C, et al. Digital breast tomosynthesis versus mammography and breast ultrasound: a multireader performance study. *Eur Radiol* 2013;23(9):2441–2449.
 123. Gur D, Rockette HE, Armfield DR, et al. Prevalence effect in a laboratory environment. *Radiology* 2003;228(1):10–14.
 124. Good WF, Abrams GS, Catullo VJ, et al. Digital breast tomosynthesis: a pilot observer study. *AJR Am J Roentgenol* 2008;190(4):865–869.
 125. Andersson I, Ikeda DM, Zackrisson S, et al. Breast tomosynthesis and digital mammography: a comparison of breast cancer visibility and BIRADS classification in a population of cancers with subtle mammographic findings. *Eur Radiol* 2008;18(12):2817–2825.
 126. Svahn T, Andersson I, Chakraborty D, et al. The diagnostic accuracy of dual-view digital mammography, single-view breast tomosynthesis and a dual-view combination of breast tomosynthesis and digital mammography in a free-response observer performance study. *Radiat Prot Dosimetry* 2010;139(1-3):113–117.
 127. Hakim CM, Chough DM, Ganott MA, Sumkin JH, Zuley ML, Gur D. Digital breast tomosynthesis in the diagnostic environment: A subjective side-by-side review. *AJR Am J Roentgenol* 2010;195(2):W172–W176.
 128. Tingberg A, Förnvik D, Mattsson S, Svahn T, Timberg P, Zackrisson S. Breast cancer screening with tomosynthesis—initial experiences. *Radiat Prot Dosimetry* 2011;147(1-2):180–183.
 129. Förnvik D, Zackrisson S, Ljungberg O, et al. Breast tomosynthesis: accuracy of tumor measurement compared with digital mammography and ultrasonography. *Acta Radiol* 2010;51(3):240–247.
 130. Mun HS, Kim HH, Shin HJ, et al. Assessment of extent of breast cancer: comparison between digital breast tomosynthesis

- and full-field digital mammography. *Clin Radiol* 2013;68(12):1254–1259.
131. Luparia A, Mariscotti G, Durando M, et al. Accuracy of tumour size assessment in the preoperative staging of breast cancer: comparison of digital mammography, tomosynthesis, ultrasound and MRI. *Radiol Med (Torino)* 2013;118(7):1119–1136.
 132. Mariscotti G, Houssami N, Durando M, et al. Accuracy of mammography, digital breast tomosynthesis, ultrasound and MR imaging in preoperative assessment of breast cancer. *Anticancer Res* 2014;34(3):1219–1225.
 133. Mann RM, Veltman J, Barentsz JO, Wobbes T, Blickman JG, Boetes C. The value of MRI compared to mammography in the assessment of tumour extent in invasive lobular carcinoma of the breast. *Eur J Surg Oncol* 2008;34(2):135–142.
 134. Gur D, Zuley ML, Anello MI, et al. Dose reduction in digital breast tomosynthesis (DBT) screening using synthetically reconstructed projection images: an observer performance study. *Acad Radiol* 2012;19(2):166–171.
 135. Zuley ML, Bandos AI, Abrams GS, et al. Time to diagnosis and performance levels during repeat interpretations of digital breast tomosynthesis: preliminary observations. *Acad Radiol* 2010;17(4):450–455.
 136. Dang PA, Freer PE, Humphrey KL, Halpern EF, Rafferty EA. Addition of tomosynthesis to conventional digital mammography: effect on image interpretation time of screening examinations. *Radiology* 2014;270(1):49–56.
 137. Reiser I, Nishikawa RM, Giger ML, et al. Computerized mass detection for digital breast tomosynthesis directly from the projection images. *Med Phys* 2006;33(2):482–491.
 138. Chan HP, Wei J, Zhang Y, et al. Computer-aided detection of masses in digital tomosynthesis mammography: comparison of three approaches. *Med Phys* 2008;35(9):4087–4095.
 139. Chan HP, Wei J, Sahiner B, et al. Computer-aided detection system for breast masses on digital tomosynthesis mammograms: preliminary experience. *Radiology* 2005;237(3):1075–1080.
 140. Mazurowski MA, Lo JY, Harrawood BP, Tourassi GD. Mutual information-based template matching scheme for detection of breast masses: from mammography to digital breast tomosynthesis. *J Biomed Inform* 2011;44(5):815–823.
 141. van Schie G, Wallis MG, Leifland K, Danielsson M, Karssemeijer N. Mass detection in reconstructed digital breast tomosynthesis volumes with a computer-aided detection system trained on 2D mammograms. *Med Phys* 2013;40(4):041902.
 142. Reiser I, Nishikawa RM, Giger ML, et al. Computerized detection of mass lesions in digital breast tomosynthesis images using two- and three dimensional radial gradient index segmentation. *Technol Cancer Res Treat* 2004;3(5):437–441.
 143. Reiser I, Nishikawa RM, Edwards AV, et al. Automated detection of microcalcification clusters for digital breast tomosynthesis using projection data only: a preliminary study. *Med Phys* 2008;35(4):1486–1493.
 144. Sahiner B, Chan HP, Hadjiiski LM, et al. Computer-aided detection of clustered microcalcifications in digital breast tomosynthesis: a 3D approach. *Med Phys* 2012;39(1):28–39.
 145. Samala RK, Chan HP, Lu Y, et al. Computer-aided detection of clustered microcalcifications in multiscale bilateral filtering regularized reconstructed digital breast tomosynthesis volume. *Med Phys* 2014;41(2):021901.
 146. Viala J, Gignier P, Perret B, et al. Stereotactic vacuum-assisted biopsies on a digital breast 3D-tomosynthesis system. *Breast J* 2013;19(1):4–9.
 147. Vancanberg L, Sahbani A, Muller S, Morel G. Needle path planning for digital breast tomosynthesis biopsy using a heterogeneous model. *Robotics and Automation (ICRA)*. IEEE International Conference, 2011; 5749–5755.
 148. Chen SC, Carton AK, Albert M, Conant EF, Schnall MD, Maidment AD. Initial clinical experience with contrast-enhanced digital breast tomosynthesis. *Acad Radiol* 2007;14(2):229–238.
 149. Carton AK, Gavenonis SC, Currihan JA, Conant EF, Schnall MD, Maidment AD. Dual-energy contrast-enhanced digital breast tomosynthesis: a feasibility study. *Br J Radiol* 2010;83(988):344–350.
 150. Schmitzberger FF, Fallenberg EM, Lawaczek R, et al. Development of low-dose photon-counting contrast-enhanced tomosynthesis with spectral imaging. *Radiology* 2011;259(2):558–564.
 151. Kapur A, Carson PL, Eberhard J, et al. Combination of digital mammography with semi-automated 3D breast ultrasound. *Technol Cancer Res Treat* 2004;3(4):325–334.
 152. Booi RC, Krücker JF, Goodsitt MM, et al. Evaluating thin compression paddles for mammographically compatible ultrasound. *Ultrasound Med Biol* 2007;33(3):472–482.
 153. Sinha SP, Goodsitt MM, Roubidoux MA, et al. Automated ultrasound scanning on a dual-modality breast imaging system: coverage and motion issues and solutions. *J Ultrasound Med* 2007;26(5):645–655.
 154. Padilla F, Roubidoux MA, Paramagul C, et al. Breast mass characterization using 3-dimensional automated ultrasound as an adjunct to digital breast tomosynthesis: a pilot study. *J Ultrasound Med* 2013;32(1):93–104.
 155. More MJ, Heng L, Goodale PJ, et al. Limited angle dual modality breast imaging. *IEEE Trans Nucl Sci* 2007;54(3):504–513.
 156. Williams MB, Judy PG, Gunn S, Majewski S. Dual-modality breast tomosynthesis. *Radiology* 2010;255(1):191–198.
 157. Li A, Miller EL, Kilmer ME, et al. Tomographic optical breast imaging guided by three-dimensional mammography. *Appl Opt* 2003;42(25):5181–5190.
 158. Fang Q, Selb J, Carp SA, et al. Combined optical and x-ray tomosynthesis breast imaging. *Radiology* 2011;258(1):89–97.
 159. Vedantham S, Shi L, Karellas A, et al. Semi-automated segmentation and classification of digital breast tomosynthesis reconstructed images. *Conf Proc IEEE Eng Med Biol Soc* 2011;2011:6188–6191.
 160. Krishnaswamy V, Michaelsen KE, Pogue BW, et al. A digital x-ray tomosynthesis coupled near infrared spectral tomography system for dual-modality breast imaging. *Opt Express* 2012;20(17):19125–19136.
 161. Kopans DB. Digital breast tomosynthesis: a better mammogram. *Radiology* 2013;267(3):968–969.
 162. Lee CI, Lehman CD. Digital breast tomosynthesis and the challenges of implementing an emerging breast cancer screening technology into clinical practice. *J Am Coll Radiol* 2013;10(12):913–917.
 163. Lee CI, Cevik M, Alagoz O, et al. Comparative effectiveness of combined digital mammography and tomosynthesis screening for women with dense breasts. *Radiology* 2015;274(3):772–780.